Experimental study of photoactivation in proton-enriched ^{113}In, ^{112}Sn, and ^{114}Sn nuclei and their contribution to the γ-process

Anastasiia Chekhovska[1,2], Yevgen Skakun[2], Igor Semisalov[2]
Sunghoon Ahn[1], Soonchul Choi[1]

[1] Institute for Basic Science, Center for Exotic Nuclear Studies (IBS, CENS), South Korea.
[2] National Scientific Center "Kharkiv Institute of Physics and Technology" (NSC KIPT), Ukraine.

Motivation (1)

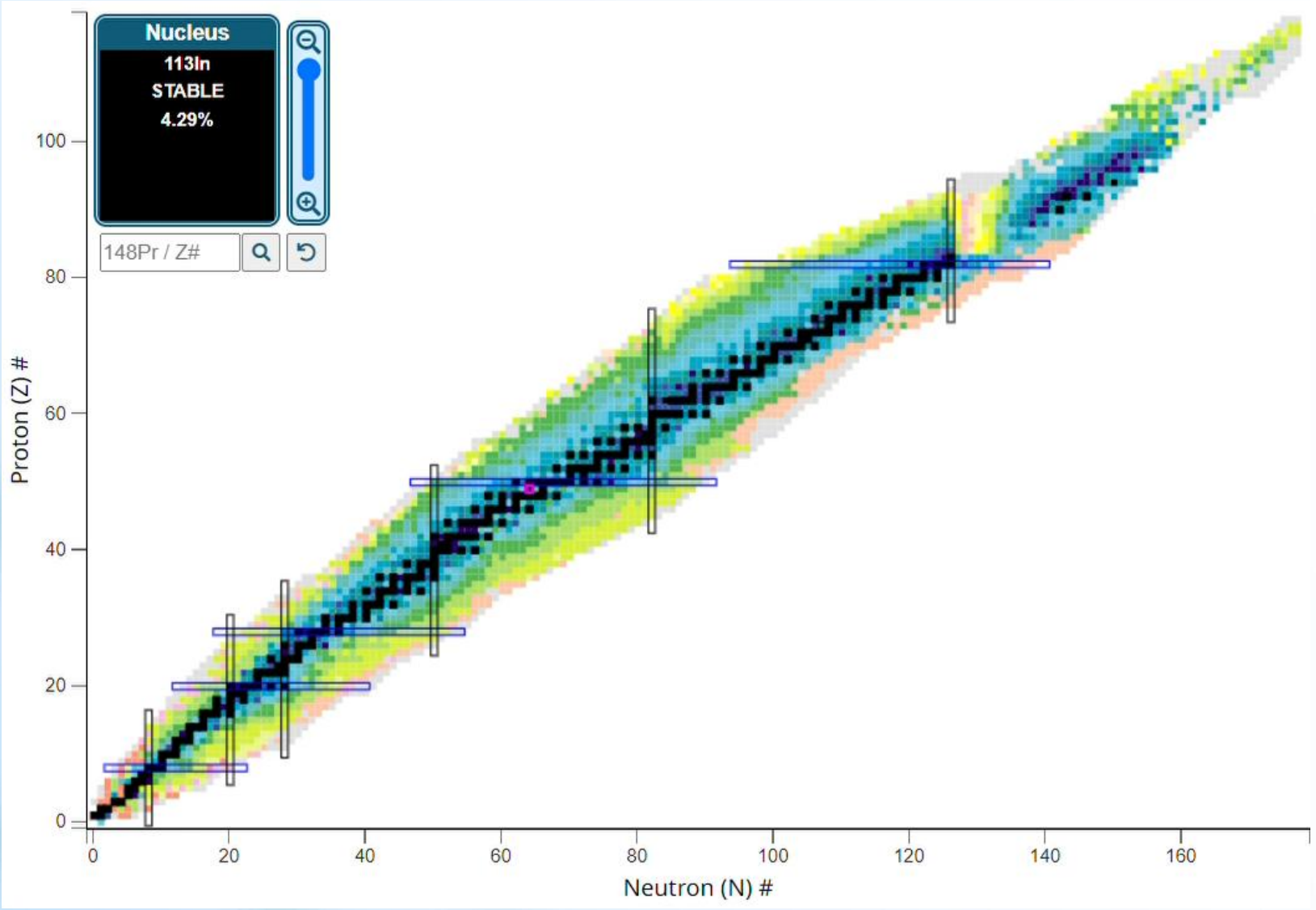

Motivation (2)

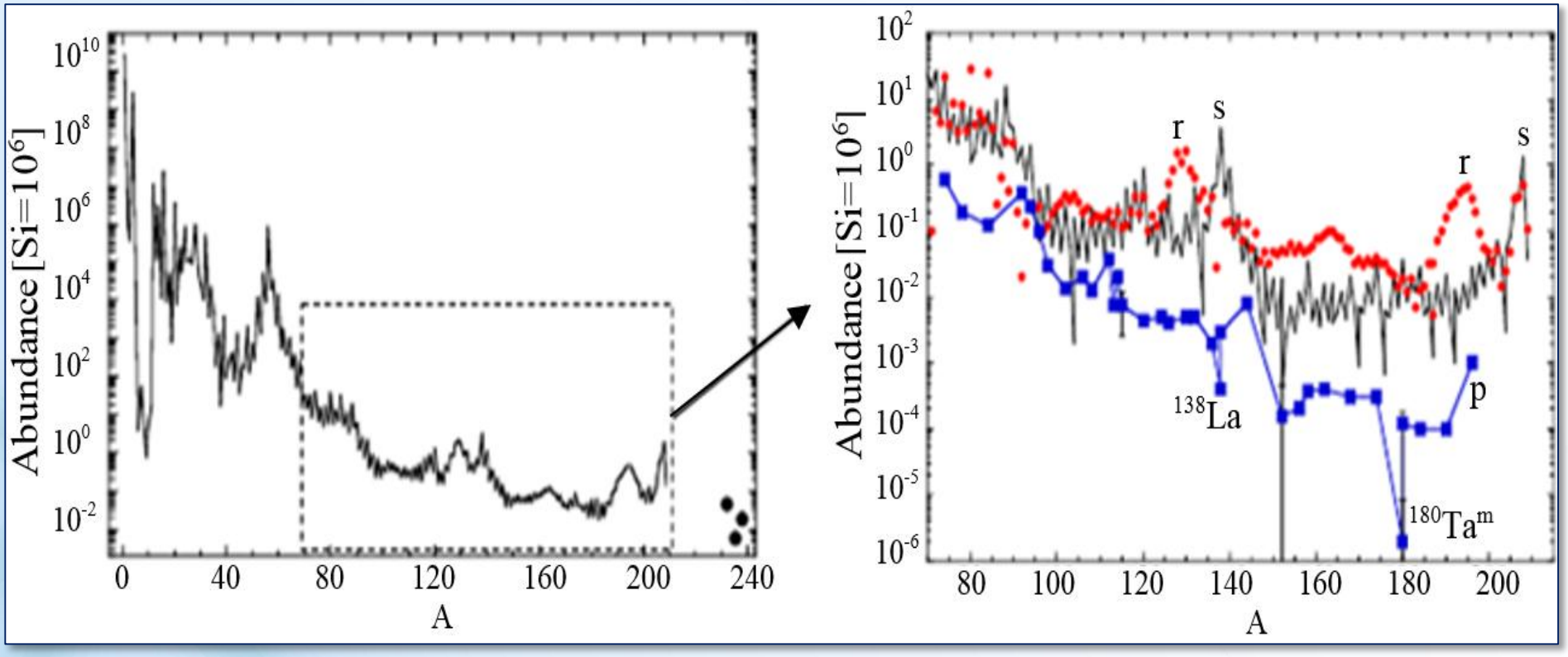

List of p-nuclei

^{74}Se	^{78}Kr	^{84}Sr	^{92}Mo	^{94}Mo	^{96}Ru	^{98}Ru	^{102}Pd	^{106}Cd	^{108}Cd	^{113}In	^{112}Sn	^{114}Sn
^{115}Sn	^{120}Te	^{124}Xe	^{126}Xe	^{130}Ba	^{132}Ba	^{138}La	^{136}Ce	^{138}Ce	^{144}Sm	^{152}Gd	^{156}Dy	^{158}Dy
^{162}Er	^{164}Er	^{168}Yb	^{174}Hf	^{180m}Ta	^{180}W	^{184}Os	^{190}Pt	^{196}Hg				

Chain of decay and formation

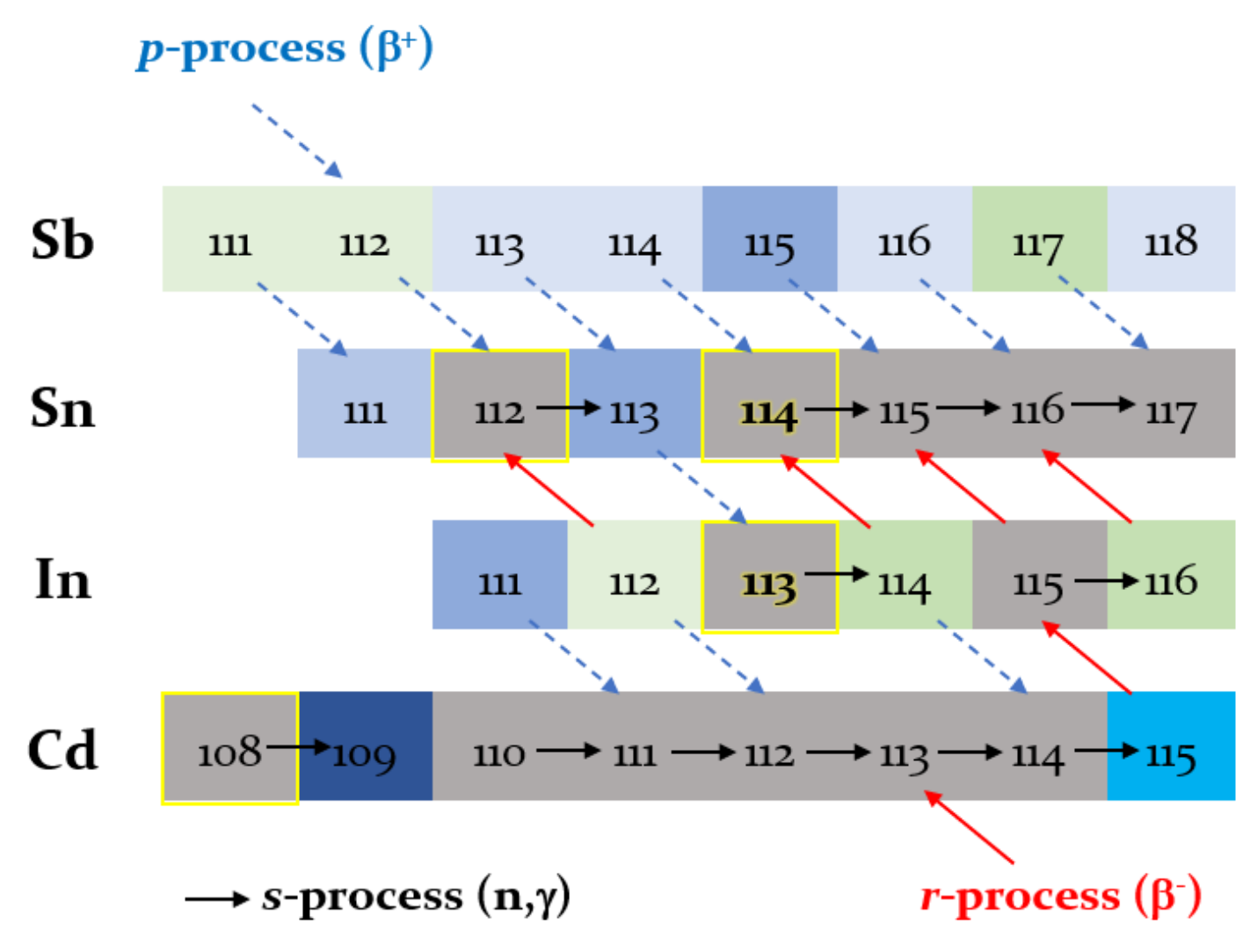

Motivation (2)

$$\lambda(T) = \int_0^{\infty} c n_\gamma(T, E_\gamma)\sigma_{(\gamma,n)}(E_\gamma)dE_\gamma$$

The reaction cross section which we obtained in the experiment

- $\lambda(T)$ – the (γ,n)-reaction rate for a nucleus disposed in a thermal photon bath of a stellar medium having temperature T;
- c – the speed of light;
- $\sigma_{(\gamma,n)}(E)$ – the reaction cross section depending on photon energy E;
- n(E,T) – the number of photons per unit energy and volume of a star interior.

Planck distribution:

$$n_\gamma(E_\gamma, T) = \left(\frac{1}{\pi}\right)^2 \left(\frac{1}{hc}\right)^3 \frac{E_\gamma^2}{\exp\left(\frac{E_\gamma}{kT}\right) - 1}$$

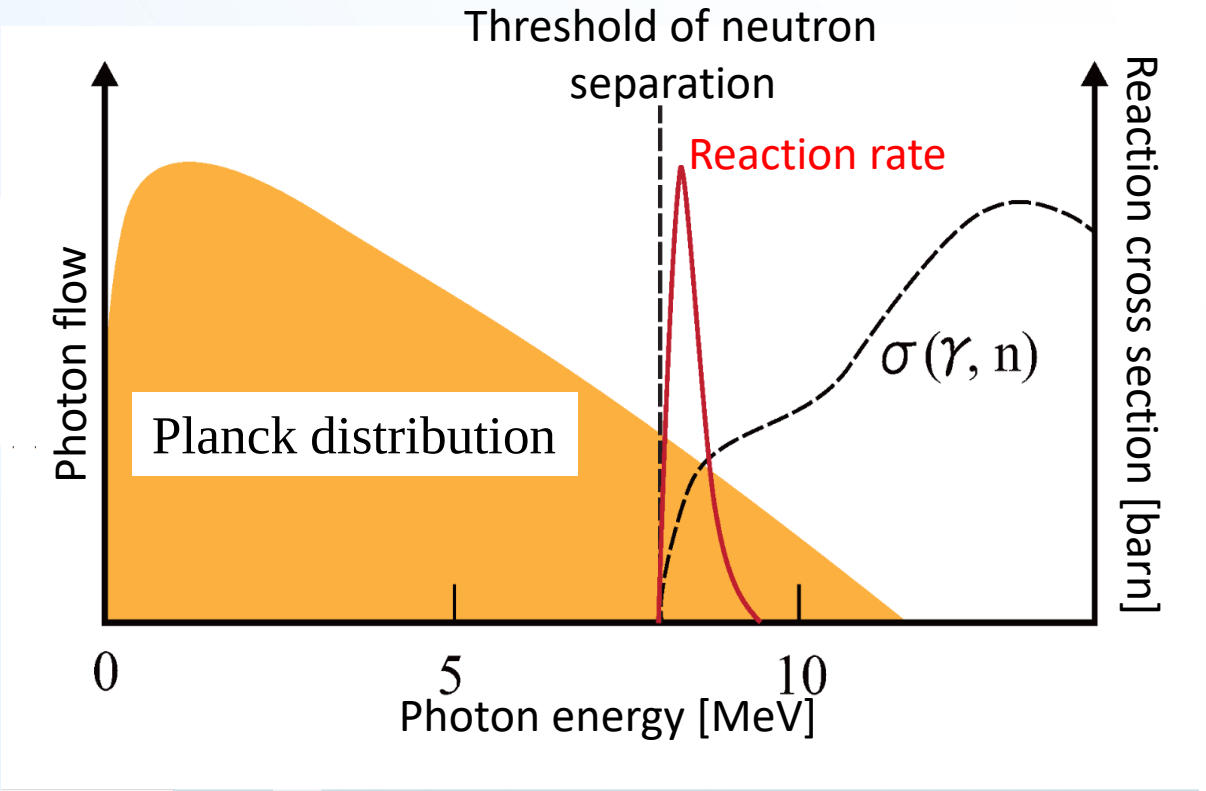

Bremsstrahlung irradiation scheme

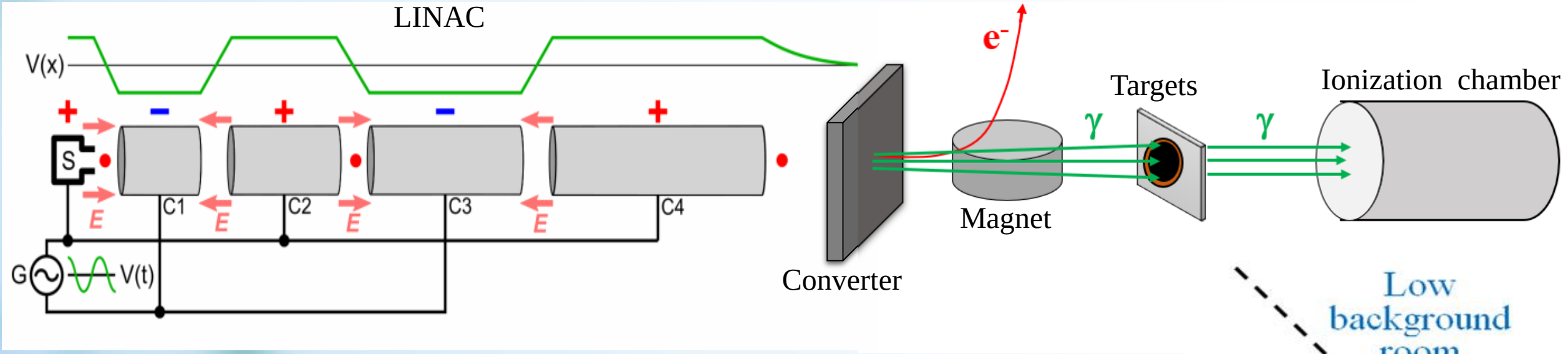

LINAC	Linear electron accelerator up to 30 MeV
Converter	Tantalum 100 μm
Magnet	Beam deflection magnet
Targets	^{113}In (79%), ^{112}Sn (80%), ^{114}Sn (83%) + monitor ^{197}Au
Ionization chamber	Used as a monitor to control bremsstrahlung flux
Detector	HP(Ge) detector Canberra

Dependence of the intensity of the photon flow on time

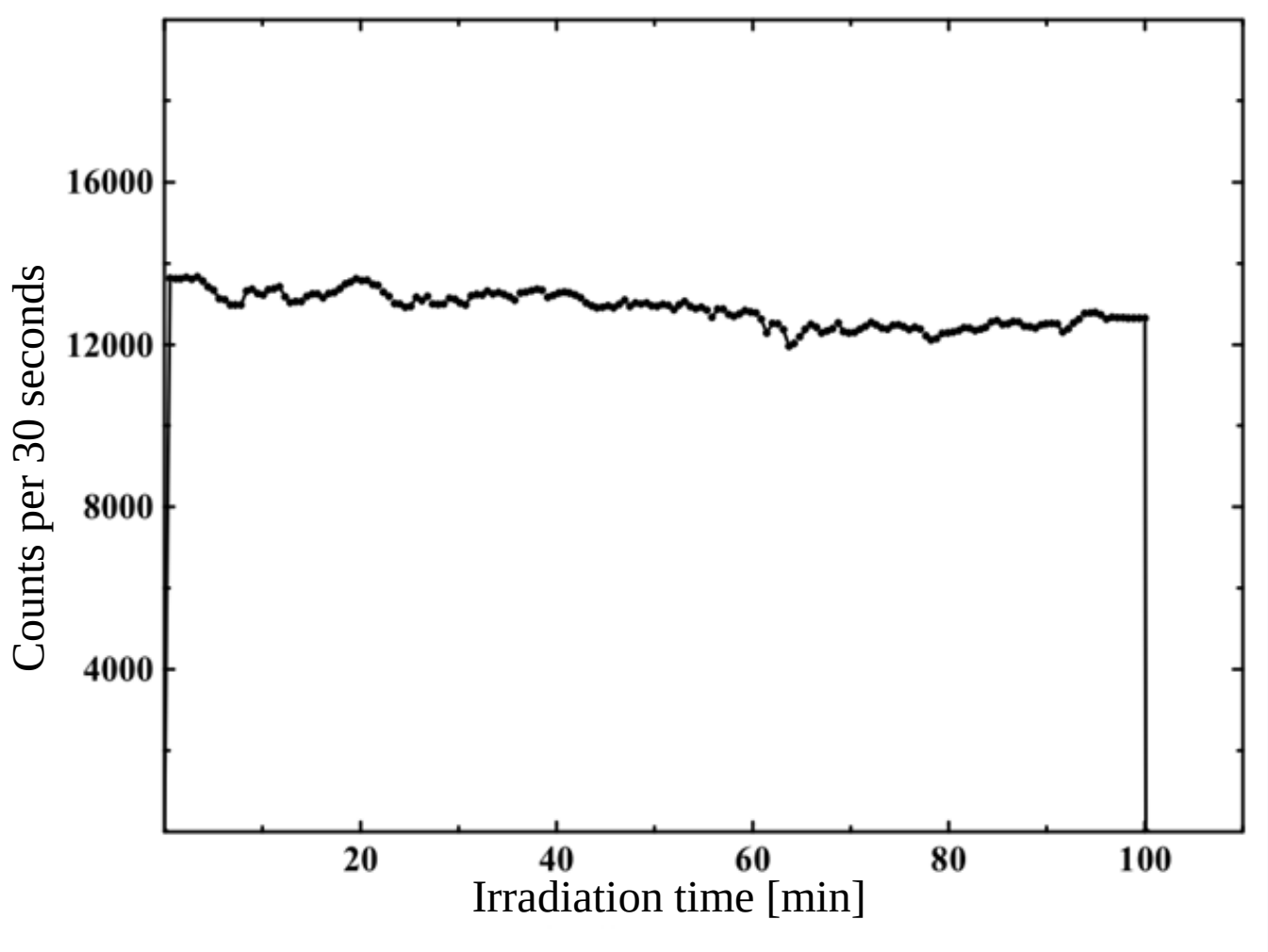

* Chekhovska A., Skakun Y., Semisalov I., Kasilov V. “Intensities of the strongest γ-ray transitions originating from the ^{111}Sn decay determined via photoactivation yield measurements” // Nuclear Instruments and Methods in Physics Research Section B: Beam Interactions with Materials and Atoms, 2022. Vol. 517. P. 1-5.

HPGe detector

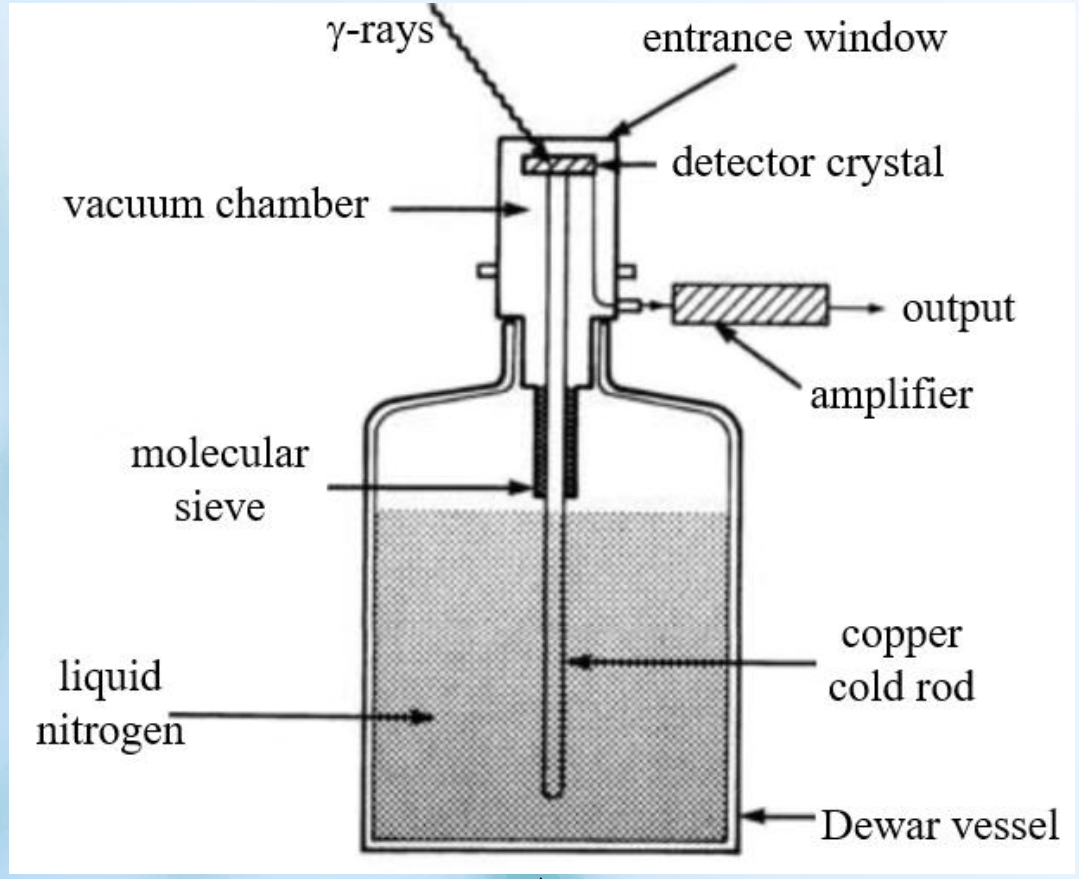

Efficiency = 30%
Resolution = 1.8 keV

Ge(Li) detector

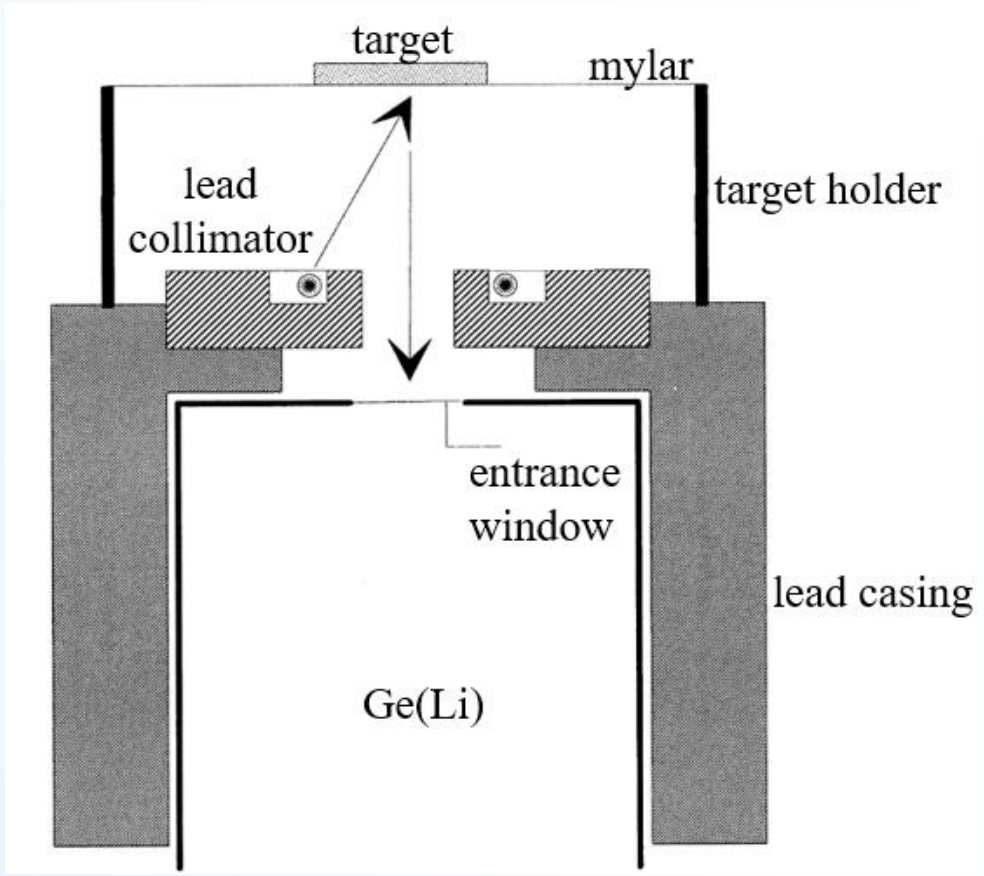

Efficiency = 20%
Resolution = 2.3 keV

Photoefficiency curves of HPGe and Ge(Li) γ-spectrometers

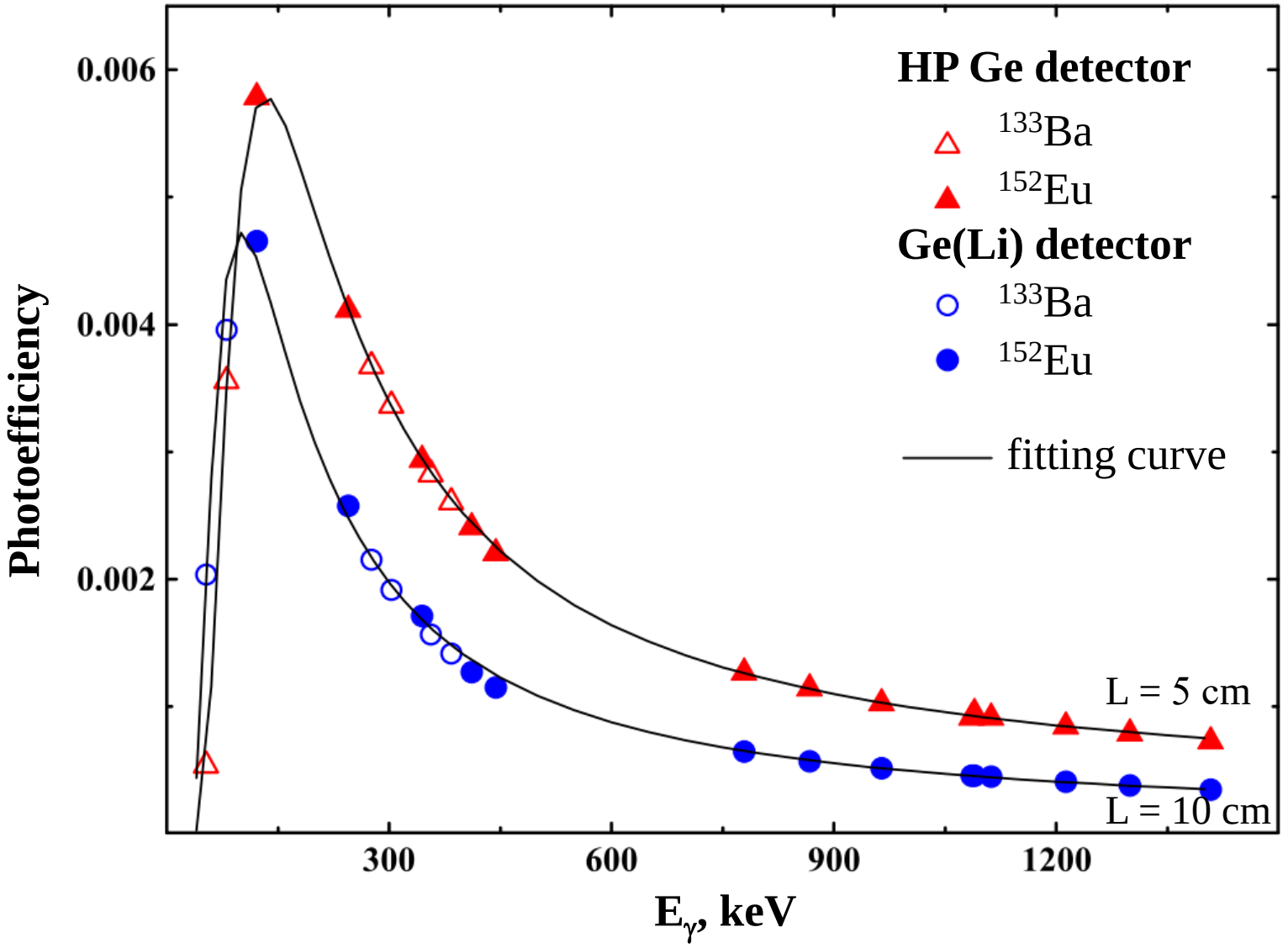

$$\ln \varepsilon_{10} = \sum_{i=1}^{3} p_i \left(\ln \frac{E}{E_0} \right) - \frac{p_4}{E^2}$$

$$\varepsilon = c_g c_p \varepsilon_{10}$$

$$c_g = \frac{2}{\pi} \int_0^1 r\, dr \int_0^\pi 1 - \left[\cos \left(\operatorname{arctg} \left(\frac{R_1}{L} \left(r \cos \varphi + \sqrt{\frac{R_2^2}{R_1^2} - r^2 sin^2\, \varphi} \right) \right) \right) \right] d\varphi$$

[Knoll, G., 2000.
Book, Radiation Detection and Measurement, 3rd edn.
John Wiley and Sons, Inc., New York, pp. 116–119.]

Efficiency calculation

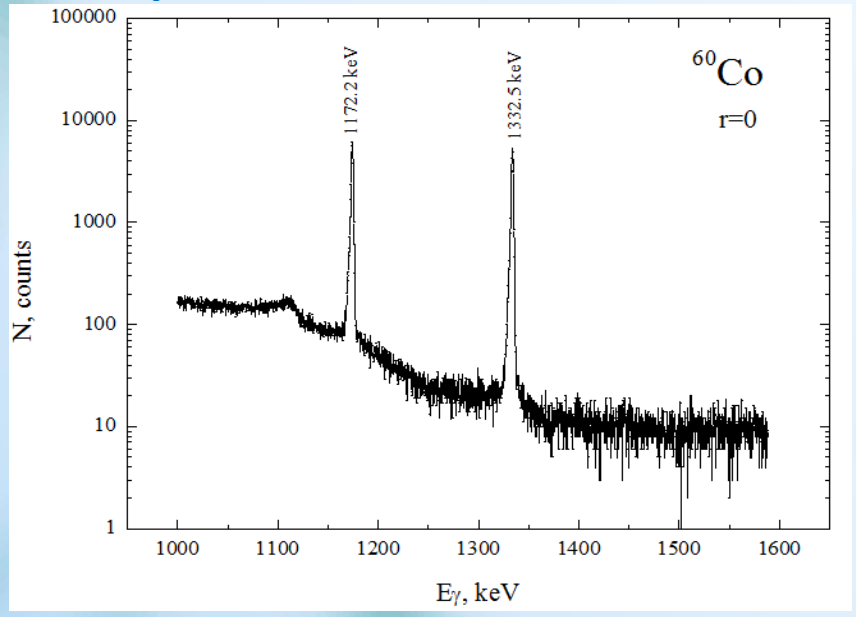

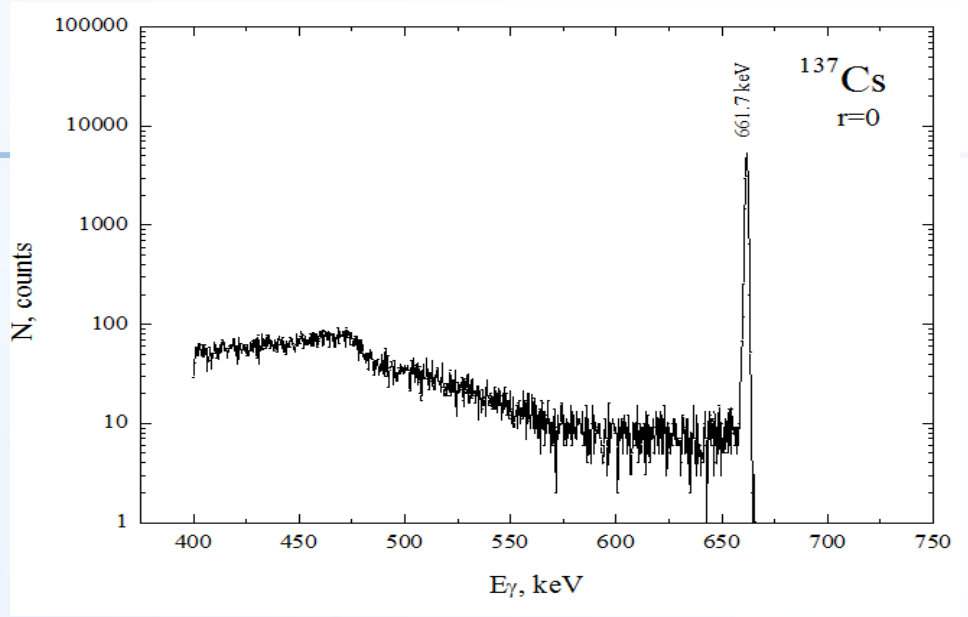

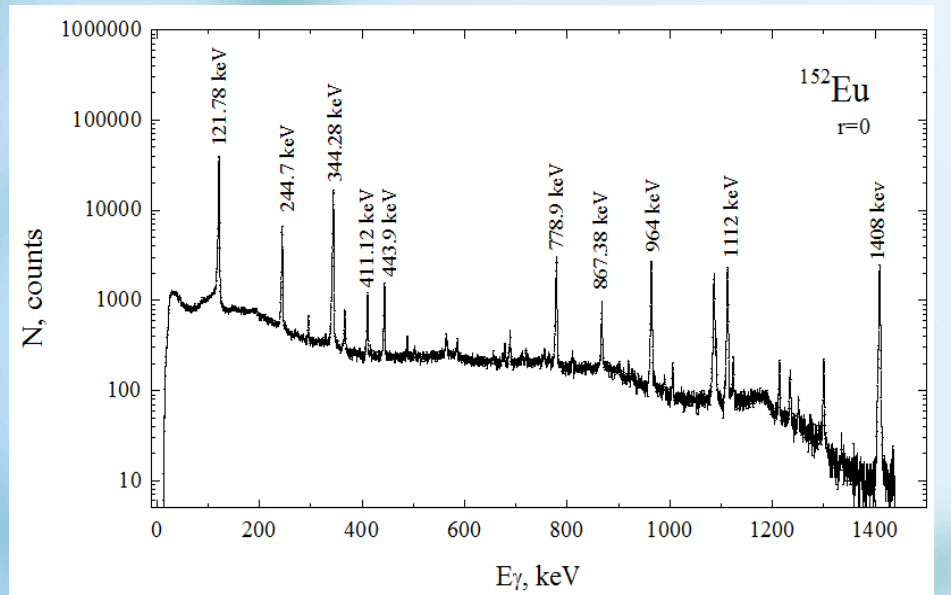

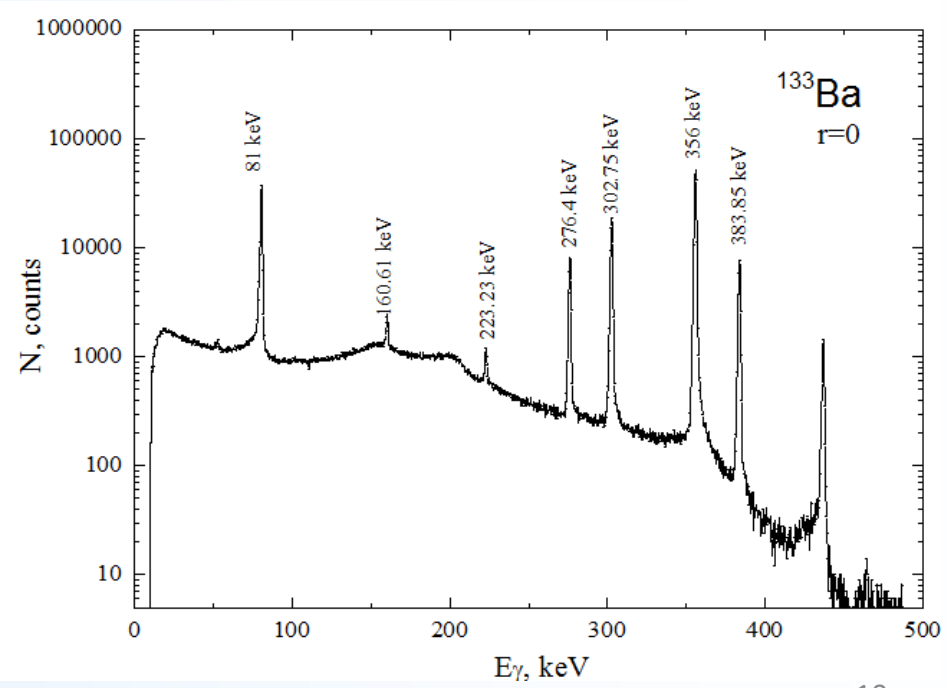

Gamma-activation method

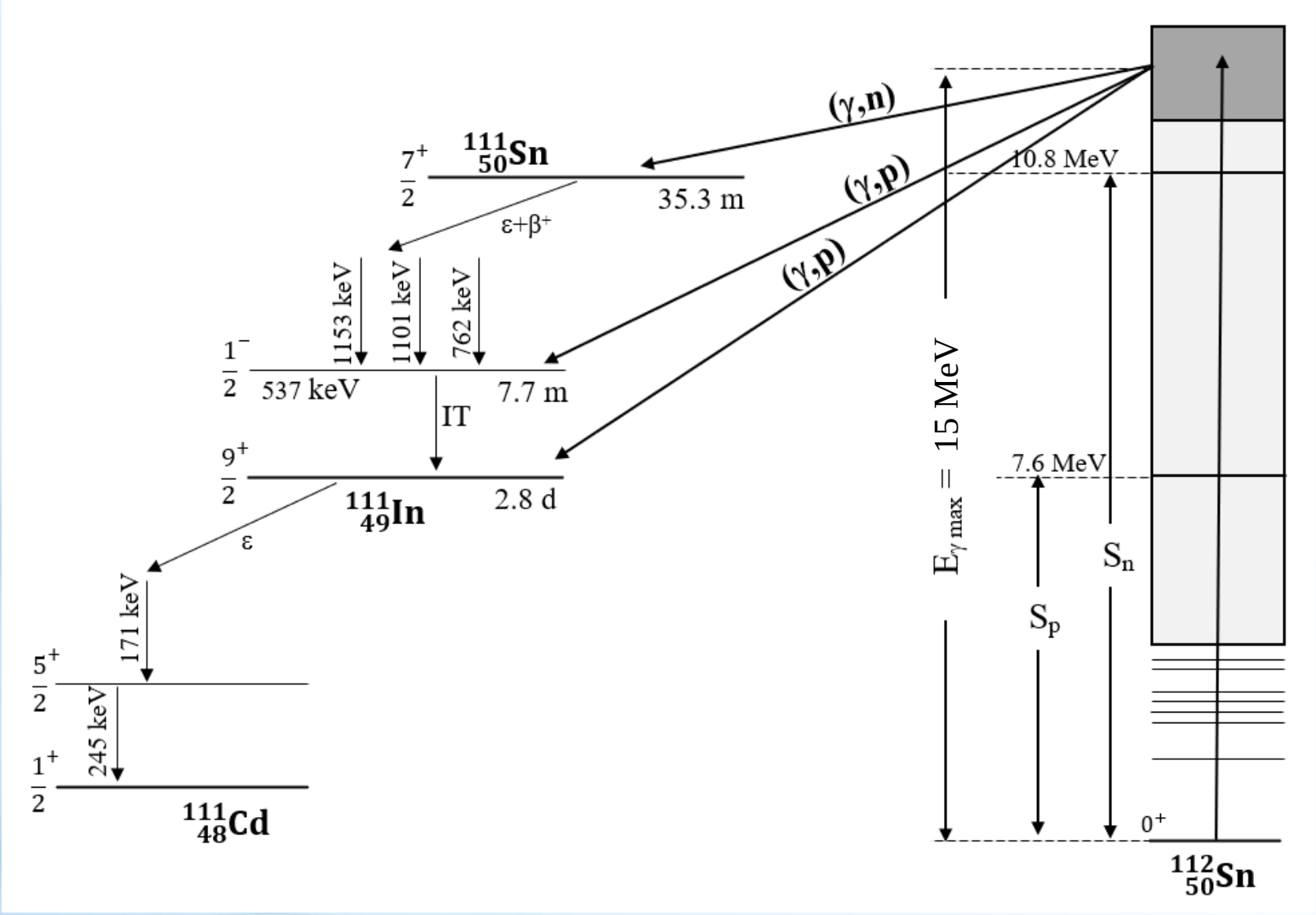

The statistical theory of nuclear reactions

- Hauser-Feshbach model:

$$\sigma_{AB} = \pi\lambda_A^2 \frac{1}{(2I+1)(2i+1)} \sum_{J^\pi} (2J+1) \frac{T_A^{J^\pi} T_B^{J^\pi}}{\sum_{A'} T_{A'}^{J^\pi}}$$

$$T_A^{J^\pi} = \sum_{i=0}^{\omega} T_A^i(J^\pi) + \int_{\varepsilon_\omega}^{\varepsilon^{max}} \sum_{J',\pi'} T_A^i(\varepsilon^i, J'\pi') \rho(\varepsilon^i, J'\pi') d\varepsilon^i$$

I - spin of the target nucleus;
i - spin of the incident particle;
J - spin of the compound nucleus;
T - coefficients of particle permeability;
ρ - nuclear levels density.

- Fermi-gas model:

$$\rho_F(E,J) = \rho_F(E) g(E,J) \approx \frac{\sqrt{\pi}}{12} \frac{\exp(2\sqrt{aE})}{a^{1/4} E^{5/4}} \frac{(2J+1)\exp\left[-\left(J+\frac{1}{2}\right)^2 / 2\sigma^2\right]}{2\sqrt{2\pi}\sigma^3}$$

E, J - the excitation and spin energies of the nucleus excited state;
a - density parameter of the levels;
σ - spin dependence parameter.

- Brink-Axel approximation:

$$f_{E1}(\varepsilon_\gamma) = 8.68 \cdot 10^{-8} (mb^{-1} MeV^{-2}) \frac{\sigma_0 \varepsilon_\gamma \Gamma^2}{\left(\varepsilon_\gamma^2 - E^2\right)^2 + \varepsilon_\gamma^2 \Gamma^2}$$

Decay curve of the ^{111}Sn isotope

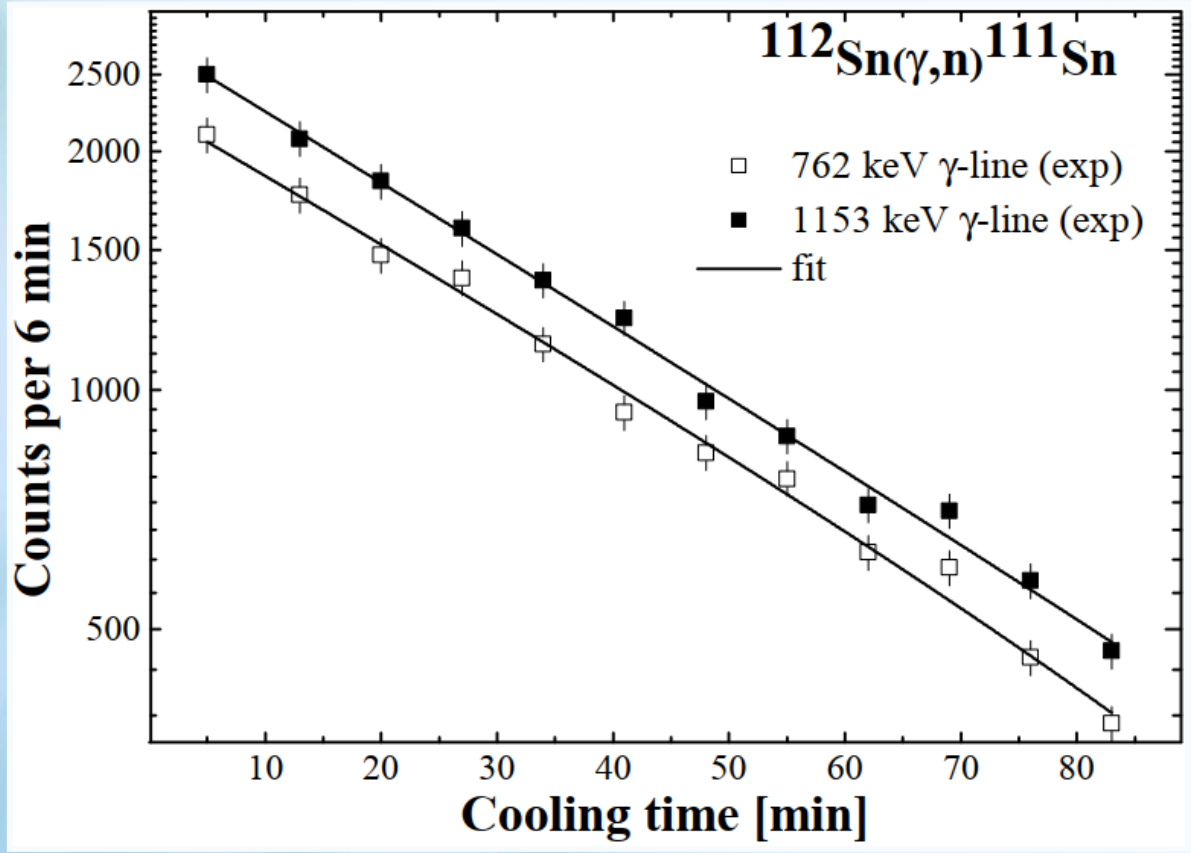

$T_{1/2}(^{111}Sn) = 35.3$ min

E_γ [keV]	I_γ [%]	Decay mode
762	1.48	e^+
1153	2.7	e^+

E_γ [keV]	I_γ [%]	Decay mode
171	90	e^+
245	94	e^+

$T_{1/2}(^{111}In) = 2.8$ d

Accumulation and decay curves of the ^{111}In isotope

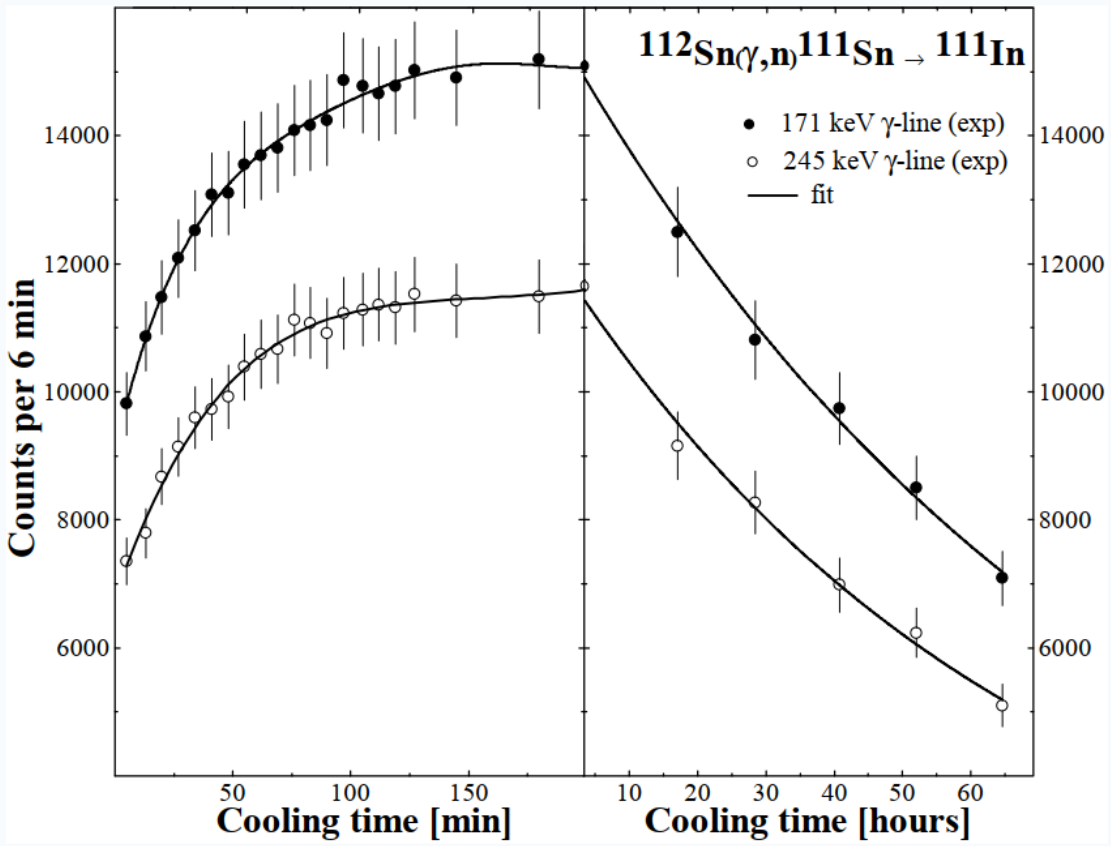

Decay of a genetic pair of radioisotopes

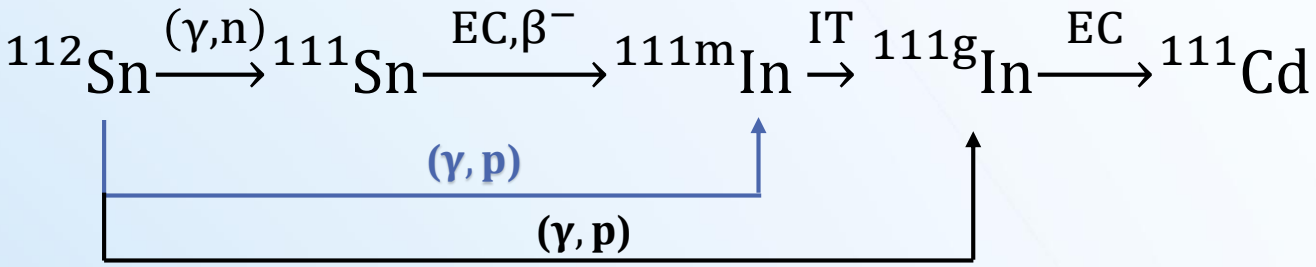

- Simple activation equation:

$$N = \frac{\varepsilon \cdot B \cdot n \cdot \phi \cdot Y}{\lambda} \cdot (1 - e^{-\lambda \cdot t_1}) \cdot e^{-\lambda \cdot t_2} \cdot (1 - e^{-\lambda \cdot t_3})$$

N – number of events
ε – efficiency
B – branching
n – number of nuclei
ϕ – incident particles flux
Y – yield

- The activation equation for genetically coupled pair:

$$Y_d = \frac{\frac{N_\gamma}{\varepsilon \cdot Br \cdot n \cdot \phi} - Y_p \cdot \frac{\lambda_p \cdot \lambda_d}{\lambda_d - \lambda_p} \cdot \left[\frac{1 - e^{-\lambda_p \cdot t_1}}{\lambda_p^2} \cdot e^{-\lambda_p \cdot t_2} \cdot \left(1 - e^{-\lambda_p \cdot t_3}\right) - \frac{1 - e^{-\lambda_d \cdot t_1}}{\lambda_d^2} \cdot e^{-\lambda_d \cdot t_2} \cdot \left(1 - e^{-\lambda_d \cdot t_3}\right) \right]}{\frac{1 - e^{-\lambda_d \cdot t_1}}{\lambda_d} \cdot e^{-\lambda_d \cdot t_2} \cdot \left(1 - e^{-\lambda_d \cdot t_3}\right)}$$

Y_p – yield of the **p**arent nuclei; Y_d – yield of the **d**aughter nuclei;
λ_p, λ_d – decay constants of the **p**arent and **d**aughter nuclei responsible;
t_1 – irradiation time; t_2 – cool time; t_3 – measure time.

TALYS 2.0

OPTICAL POTENTIAL	NUCLEAR LEVEL DENSITY	RADIATION STRENGTH FUNCTION
omp 1: Spherical OMP: Neutrons and protons; **omp 2**: Spherical dispersive OMP: Neutrons; **omp 3**: Spherical OMP: Complex particles; **omp 4**: Semi-microscopic optical model (JLM).	**ldmodel 1**: Constant Temperature + Fermi gas model (CTM) **ldmodel 2**: Back-shifted Fermi gas Model (BFM) **ldmodel 3**: Generalised Superfluid Model (GSM) **ldmodel 4**: Skyrme-Hartree-Fock-Bogolyubov level densities from numerical tables **ldmodel 5**: Skyrme-Hartree-Fock-Bogolyubov combinatorial level densities from numerical tables **ldmodel 6**: Temperature-dependent Gogny-Hartree-Fock-Bogolyubov combinatorial level densities from numerical tables	**strength 1**: Kopecky-Uhl generalized Lorentzian **strength 2**: Brink-Axel Lorentzian **strength 3**: Hartree-Fock BCS tables **strength 4**: Hartree-Fock-Bogoliubov tables **strength 5**: Goriely's hybrid model **strength 6**: Goriely T-dependent HFB **strength 7**: T-dependent RMF **strength 8**: Gogny D1M HFB+QRPA **strength 9**: SMLO **strength 10**: Skyrme HFB+QRPA

Yields of the photoneutron reaction $^{112}Sn(\gamma,n)^{111}Sn$

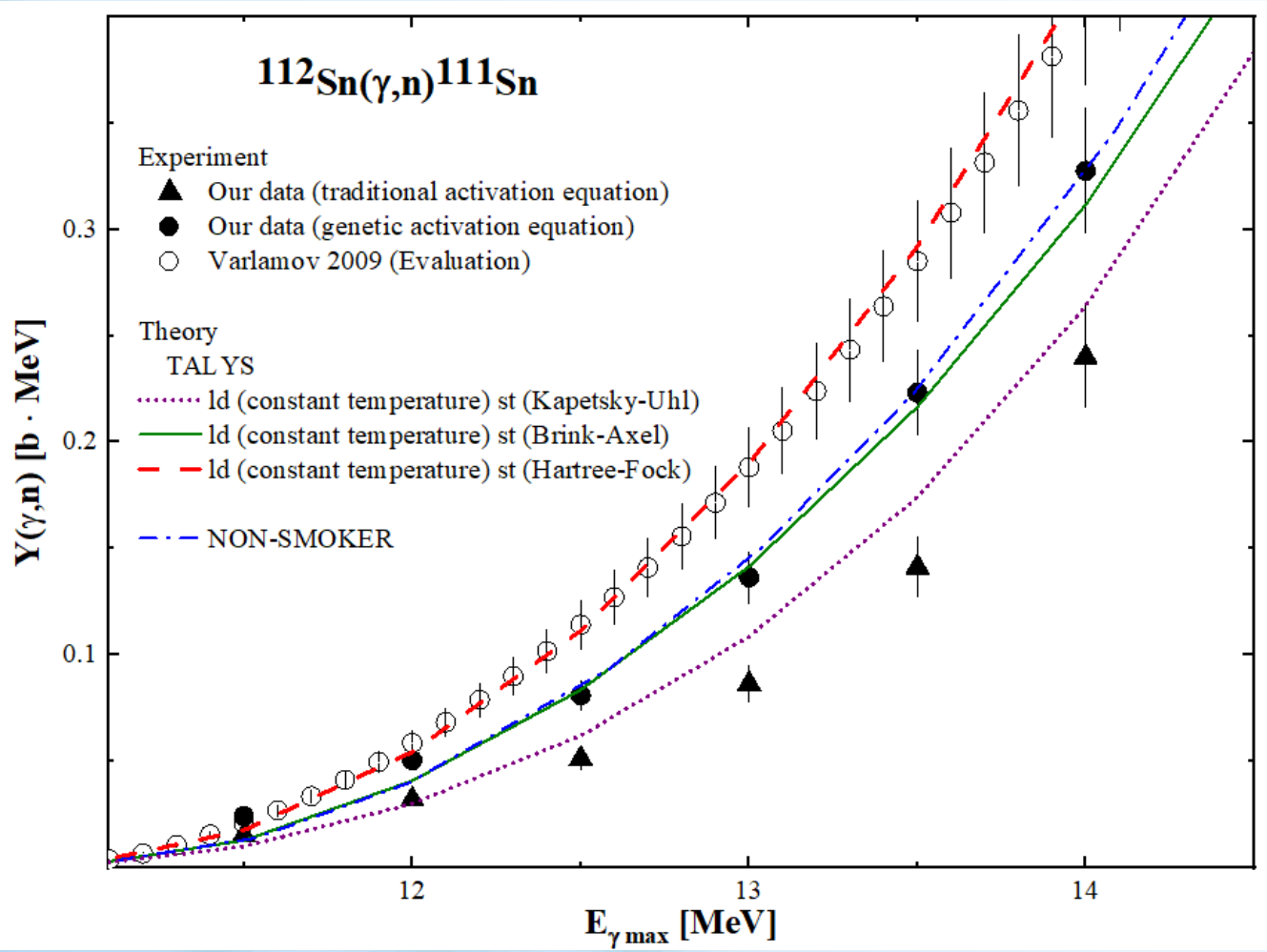

E_γ [keV]	Branching coefficient [%]	
	NUDAT	Our data
372.31	0.42 ± 0.07	0.33 ± 0.02
457.56	0.38 ± 0.06	0.27 ± 0.03
564.34	0.25 ± 0.04	0.20 ± 0.02
761.97	1.48 ± 0.23	1.09 ± 0.10
954.05	0.51 ± 0.08	0.42 ± 0.03
1101.18	0.64 ± 0.11	0.44 ± 0.05
1152.98	2.65 ± 0.4	1.90 ± 0.18
1610.47	1.31 ± 0.20	0.92 ± 0.09
1914.70	**1.38 (0.08)**	1.40 ± 0.13

* Chekhovska A., Skakun Y., Semisalov I., Kasilov V. "Intensities of the strongest γ-ray transitions originating from the ^{111}Sn decay determined via photoactivation yield measurements" // Nuclear Instruments and Methods in Physics Research Section B: Beam Interactions with Materials and Atoms, 2022. Vol. 517. P. 1-5.

CS vs RR for $^{112}Sn(\gamma,n)^{111}Sn$ reaction

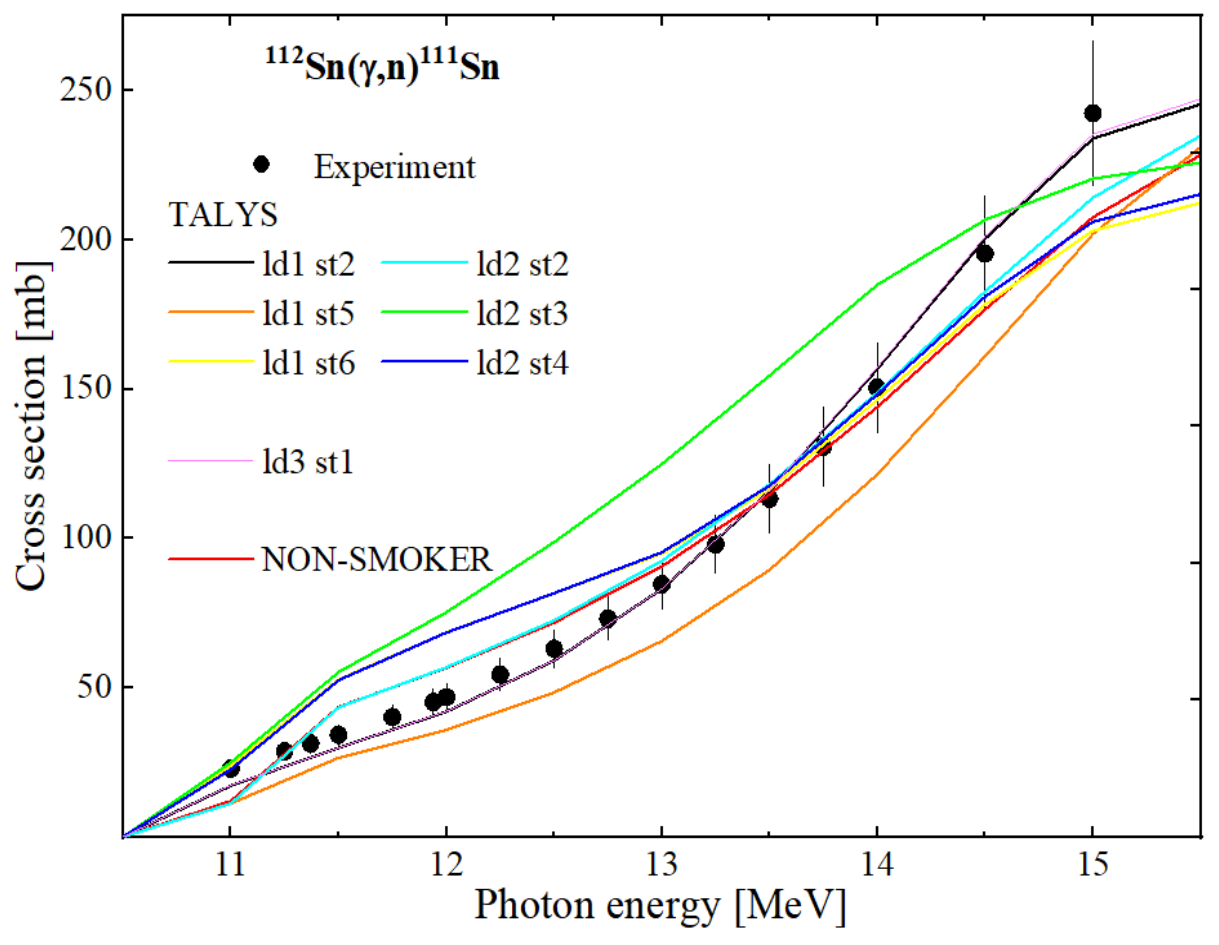

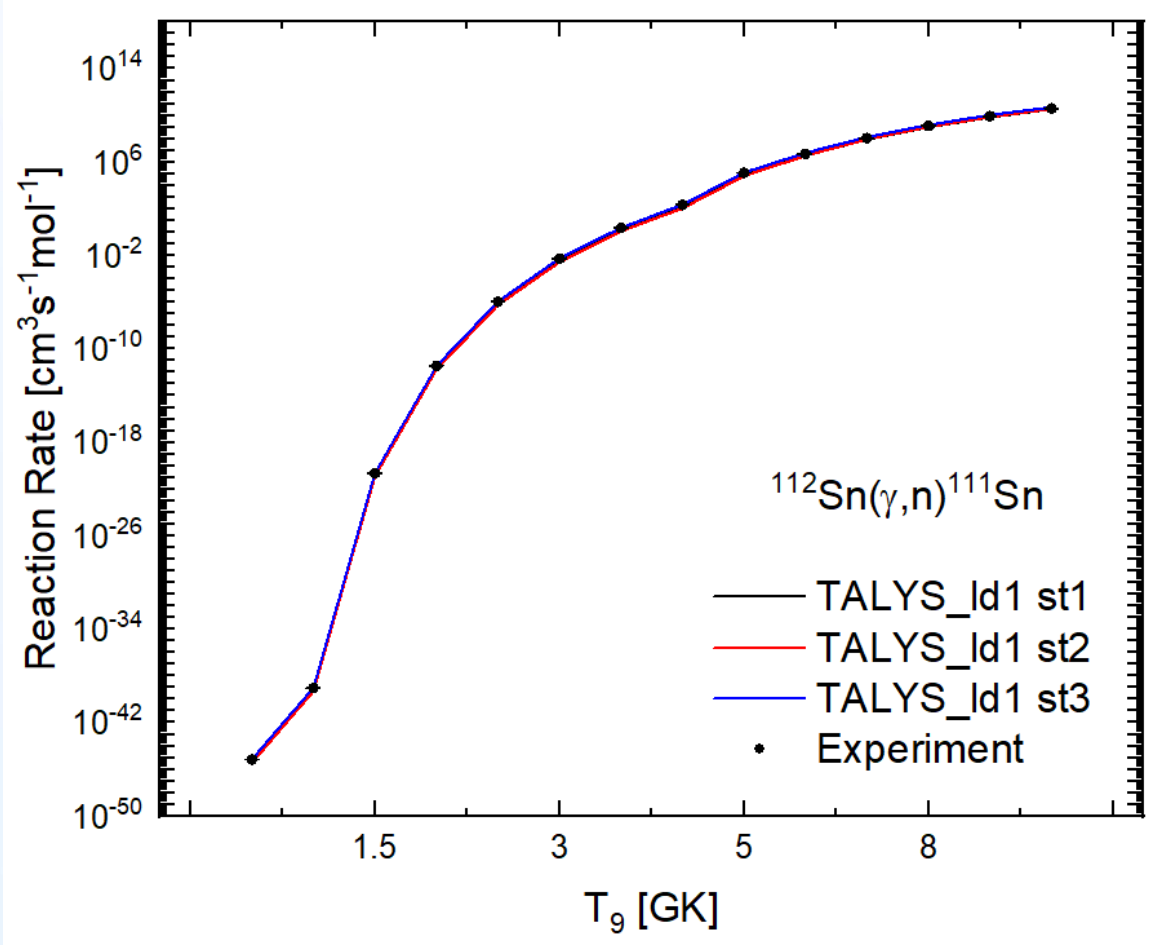

Integral cross-sections of the photonuclear reaction $^{112}Sn(\gamma,p)^{111m}In$

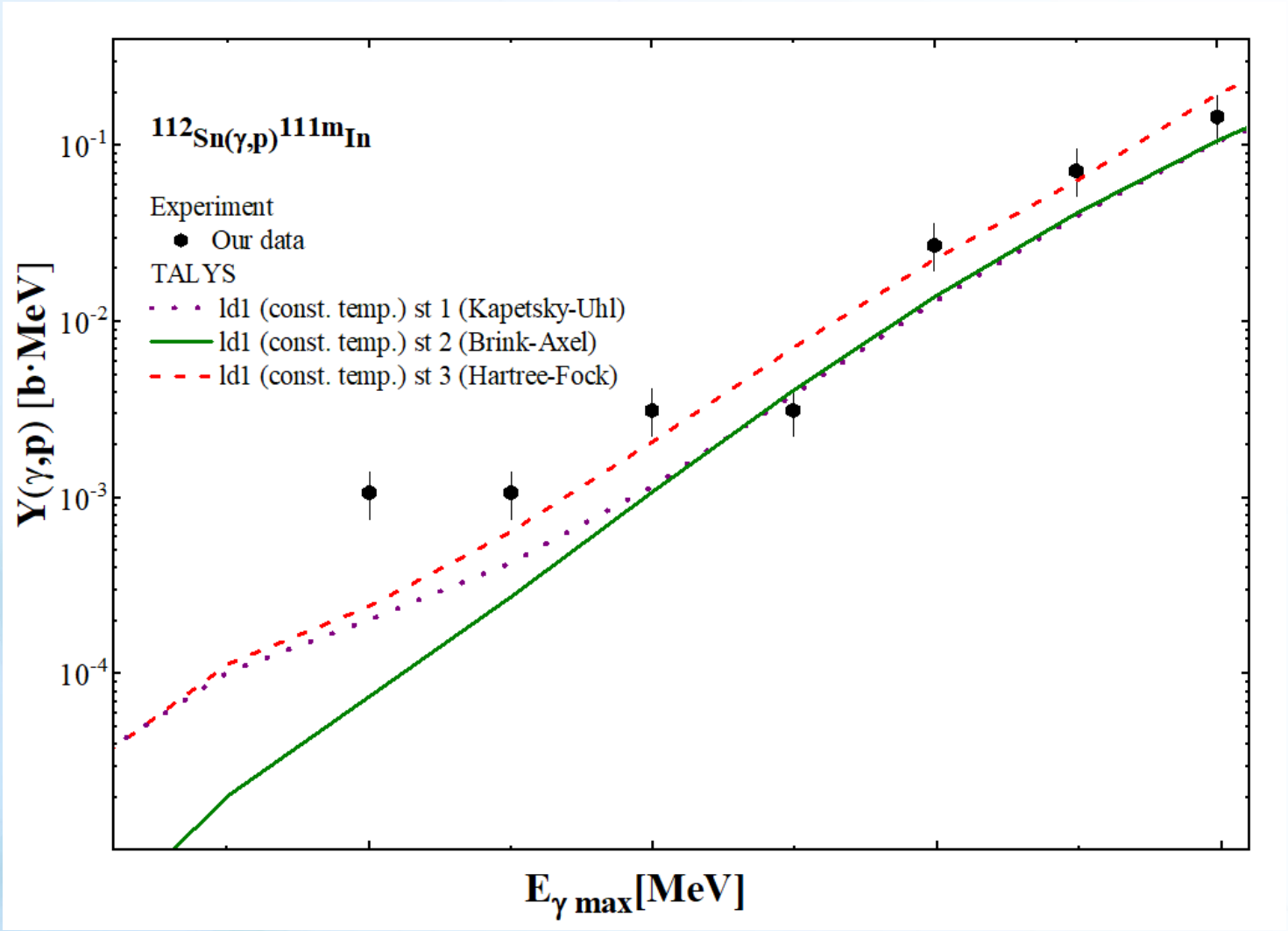

CS vs RR for $^{112}Sn(\gamma,p)^{111m}In$ reaction

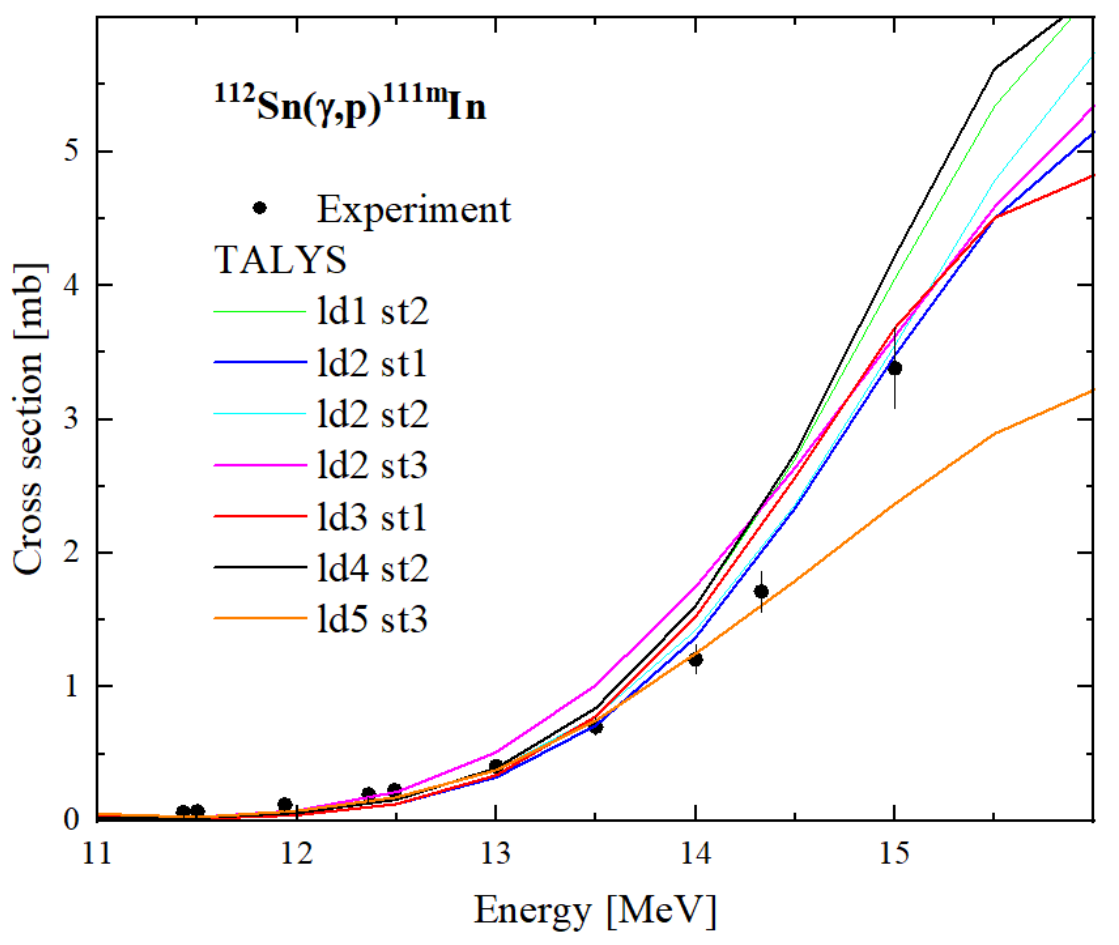

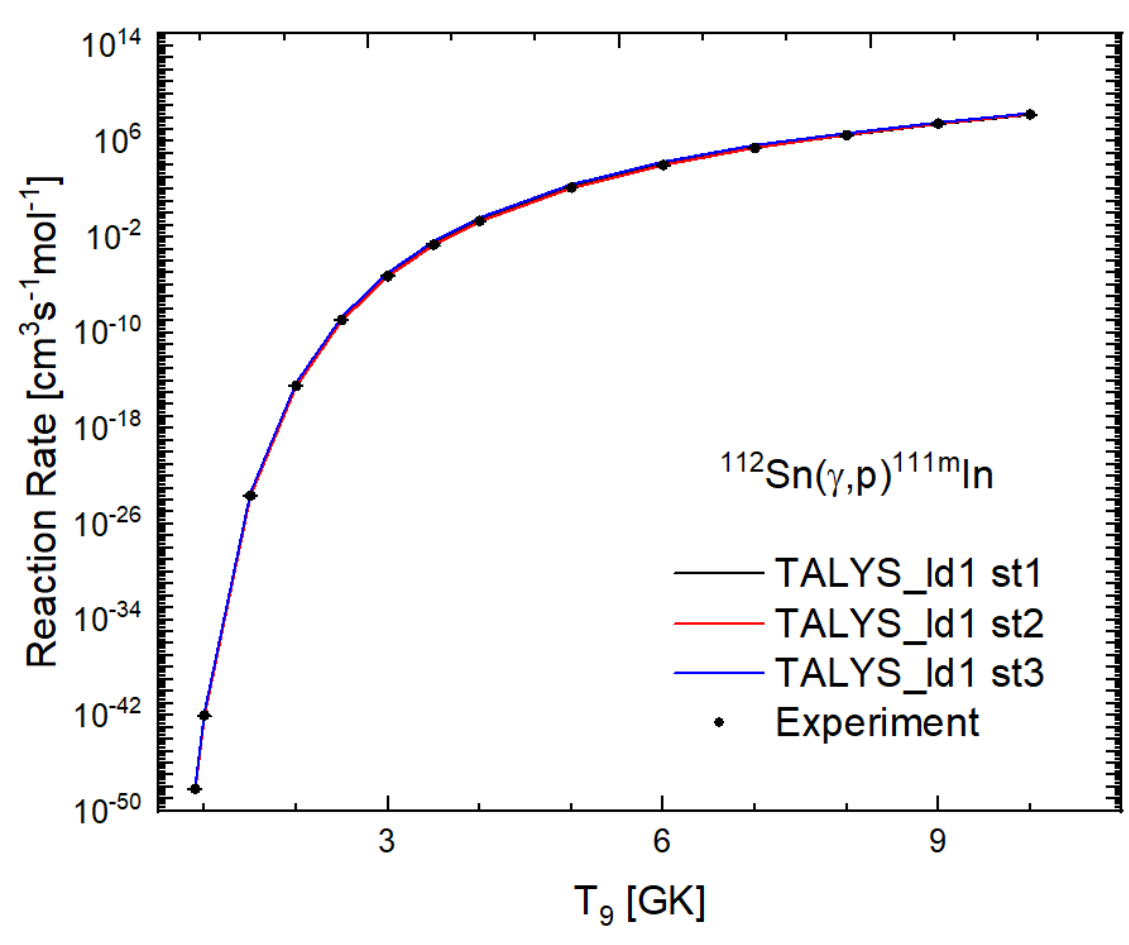

Yields of the photonuclear reaction $^{112}Sn(\gamma,p)^{111g}In$

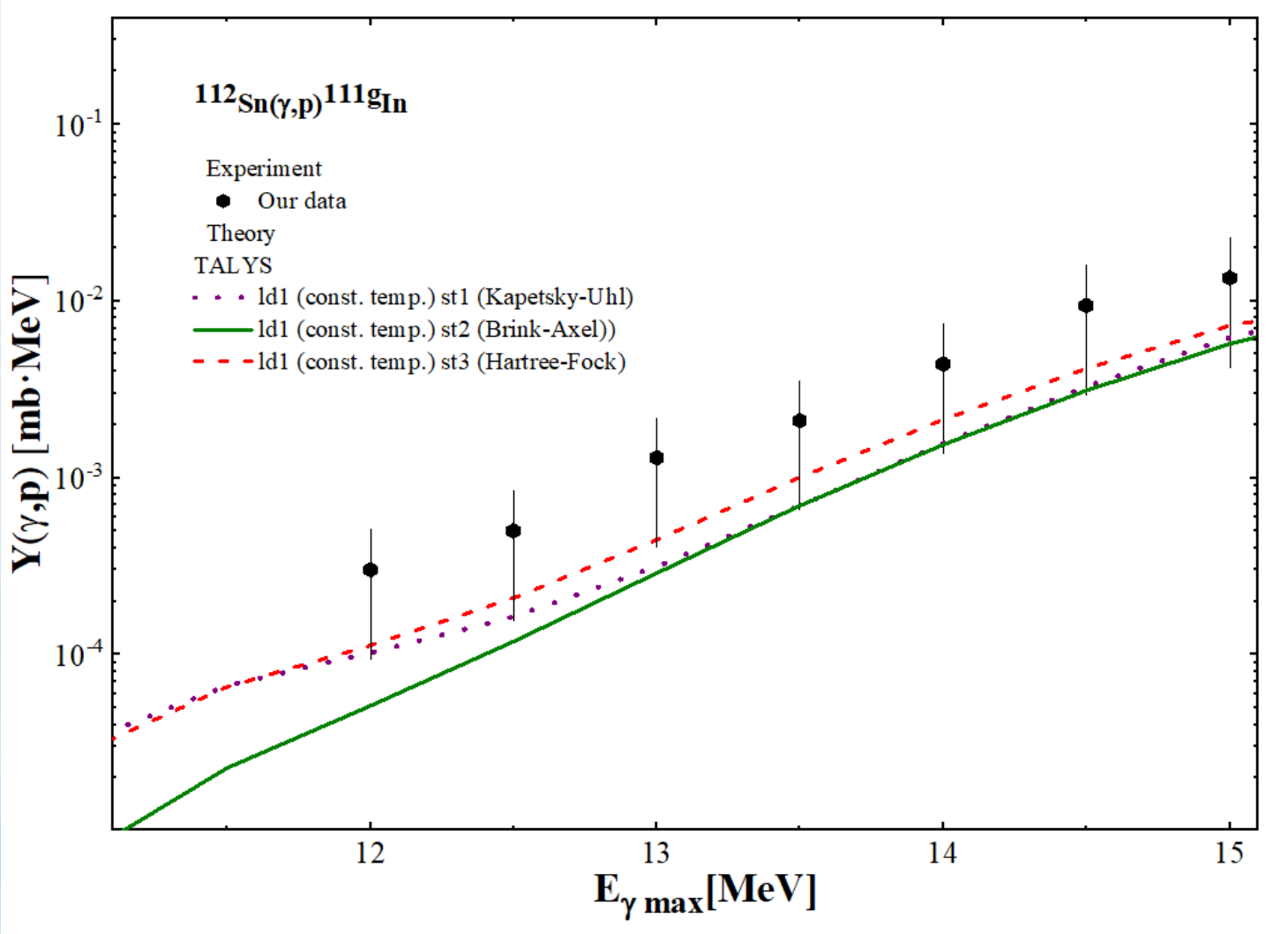

CS vs RR for $^{112}Sn(\gamma,p)^{111g}In$ reaction

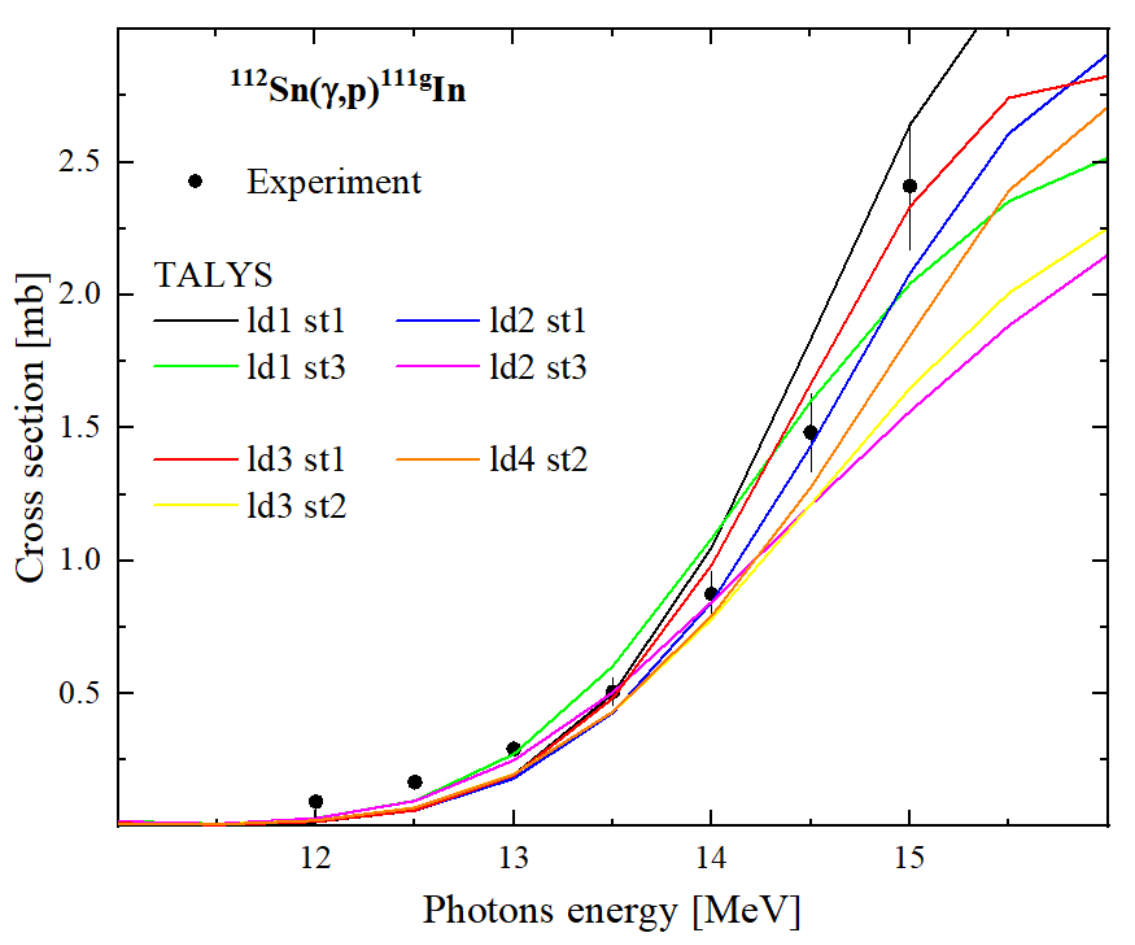

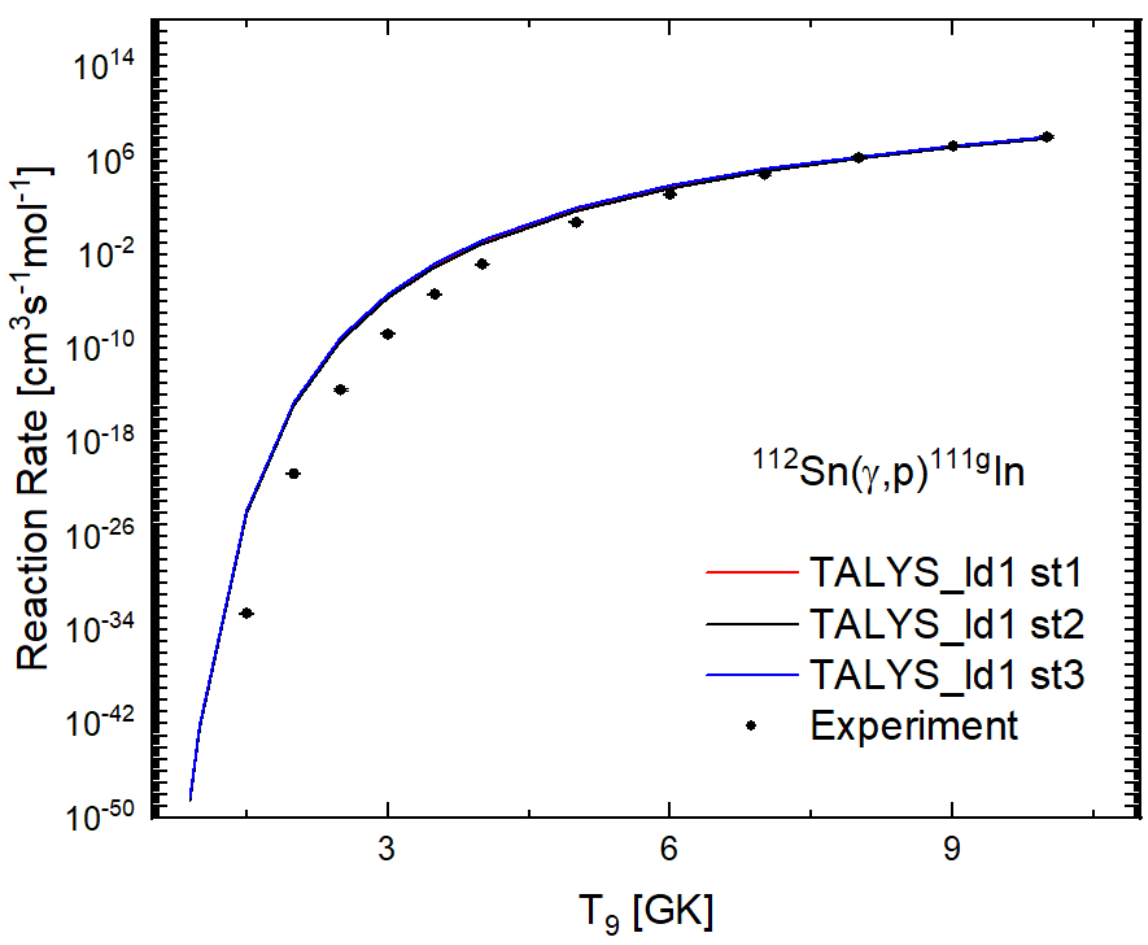

A simplified scheme of a radioactive chain $^{113}Sn \rightarrow {}^{113m,g}In$

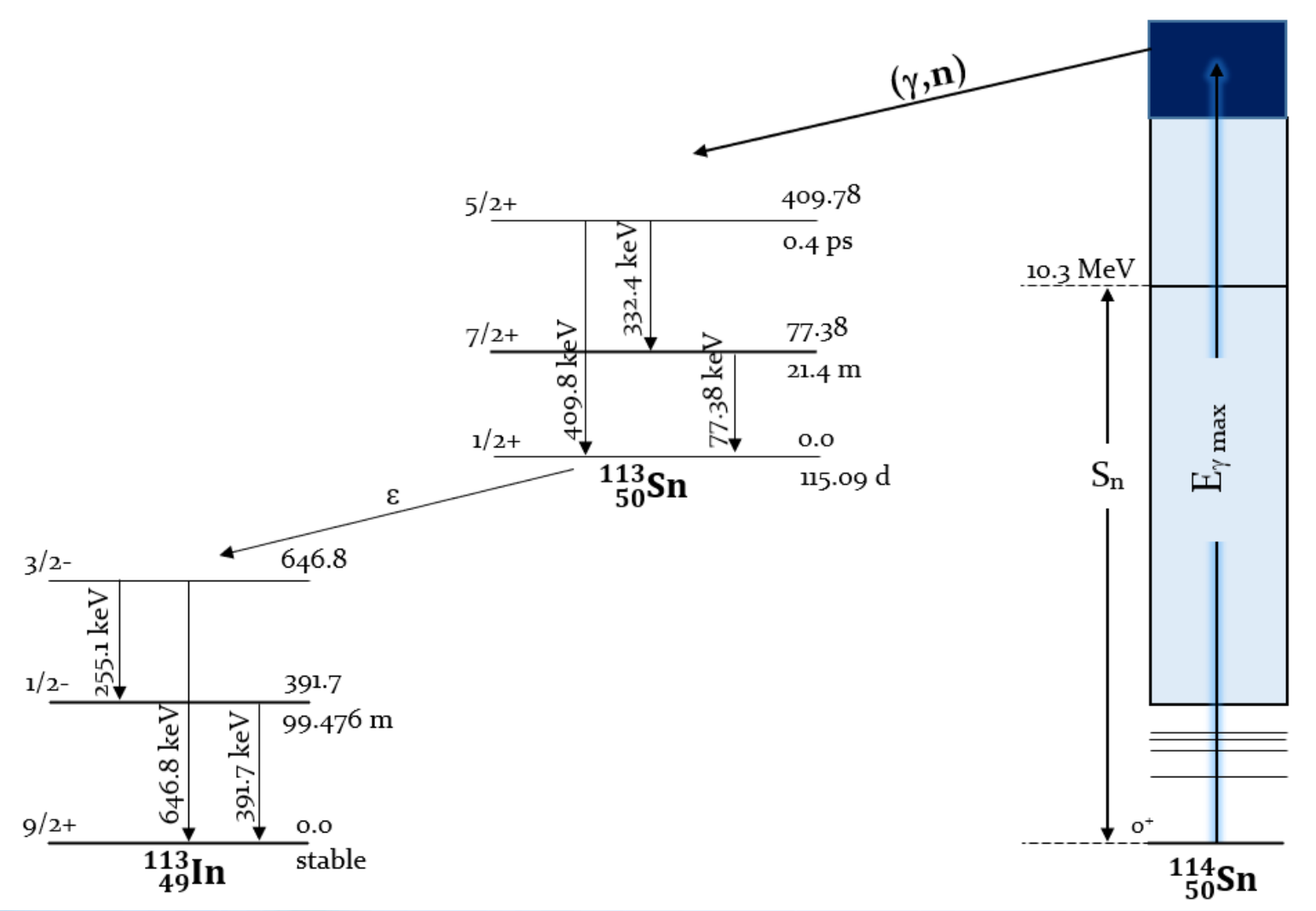

Decay spectrum from an irradiated ^{114}Sn target

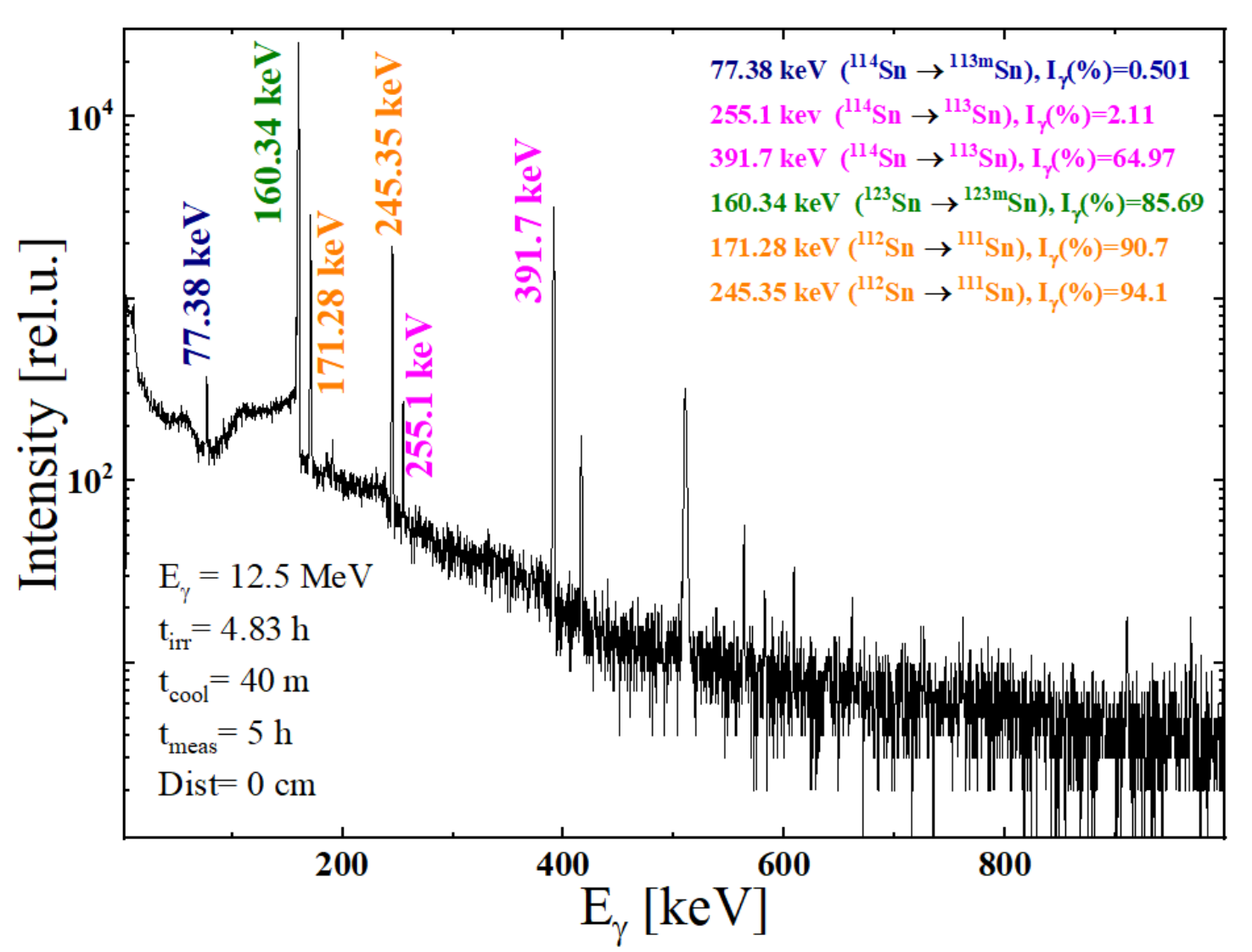

Yields of the photoneutron reaction $^{114}Sn(\gamma,n)^{113}Sn$

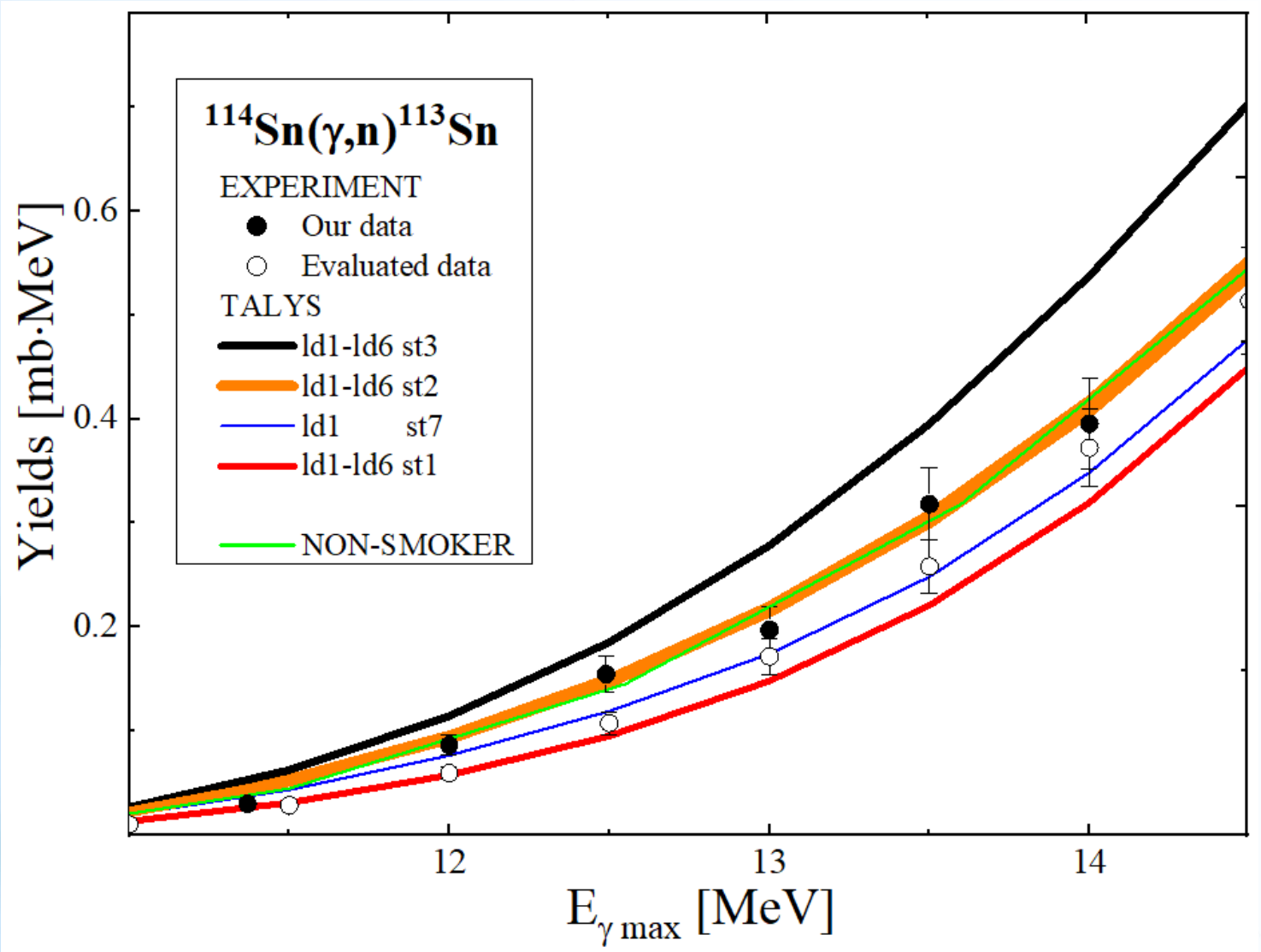

CS vs RR for $^{114}Sn(\gamma,n)^{113}Sn$ reaction

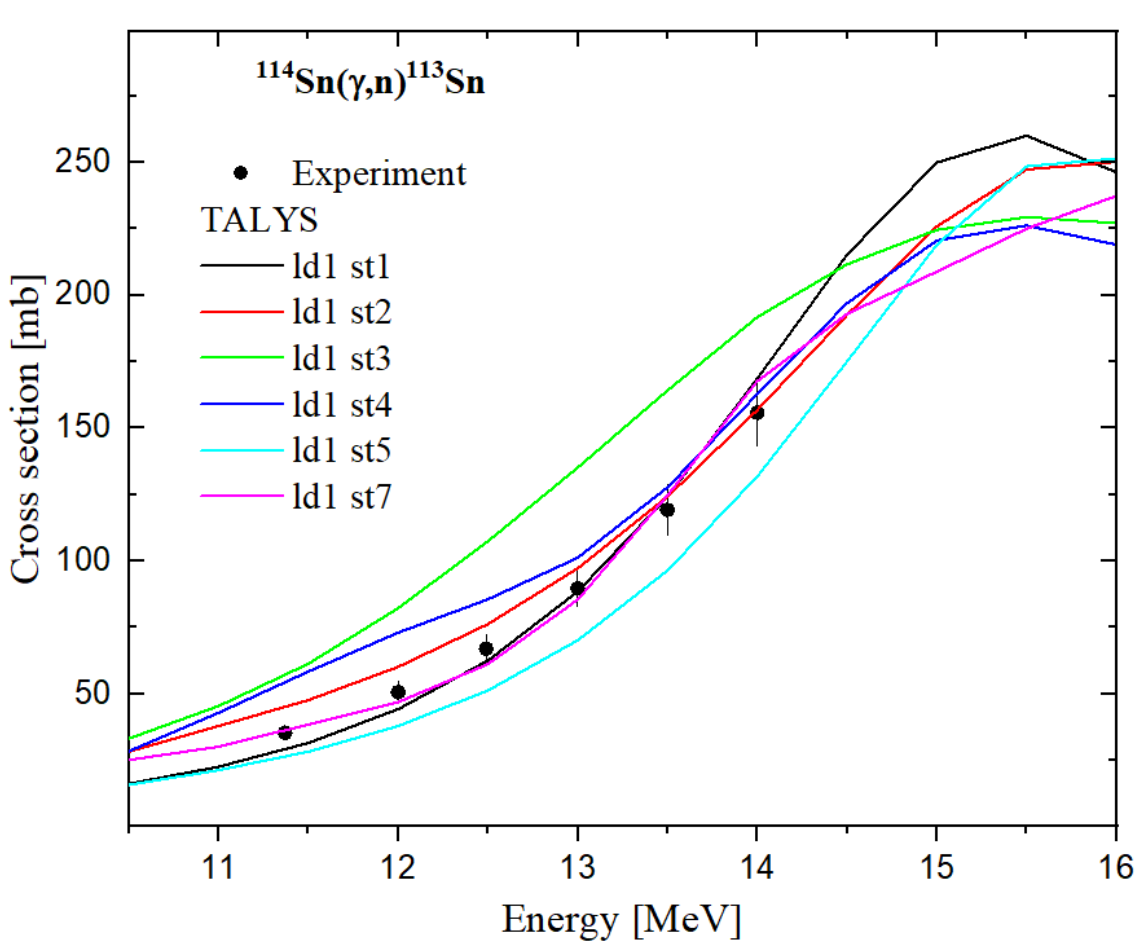

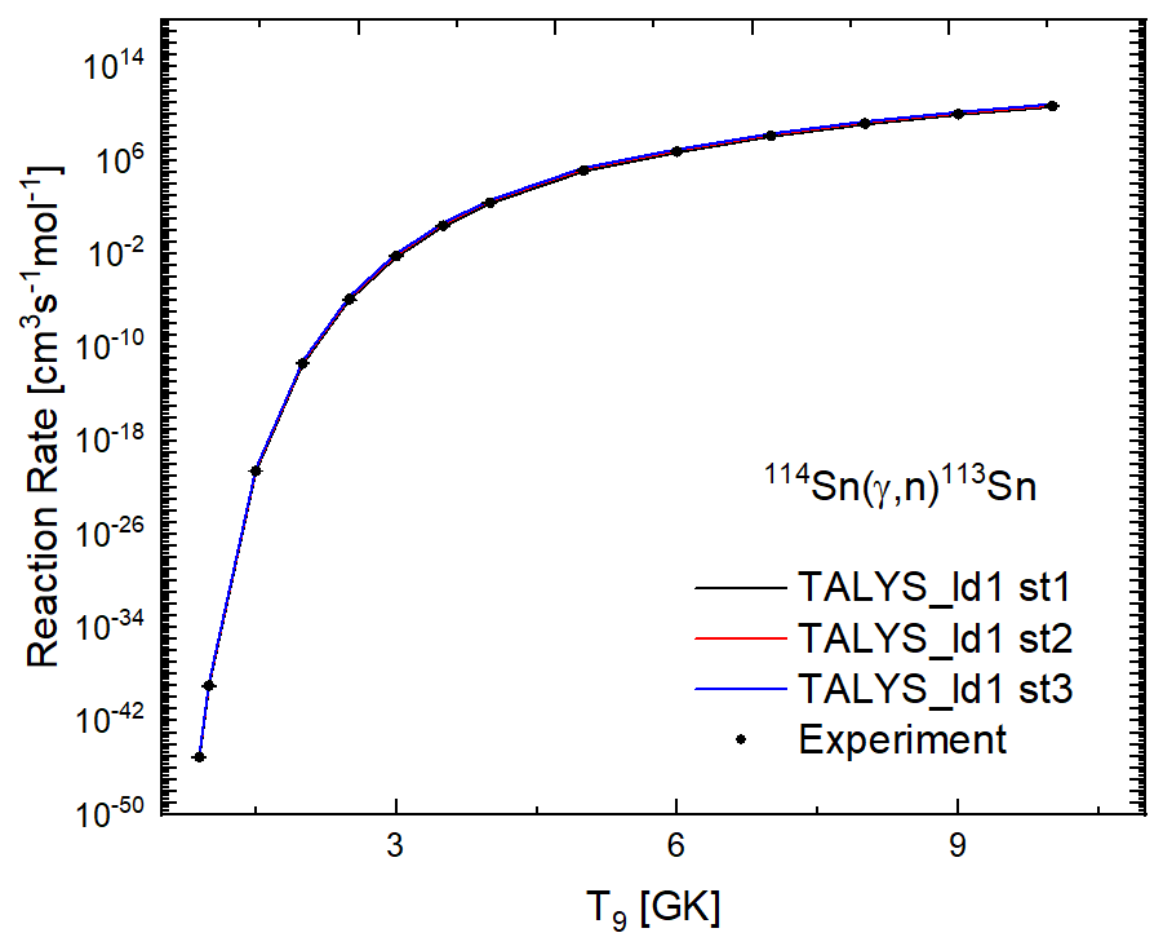

A simplified decay diagram of the isomeric pair ^{112m,g}In

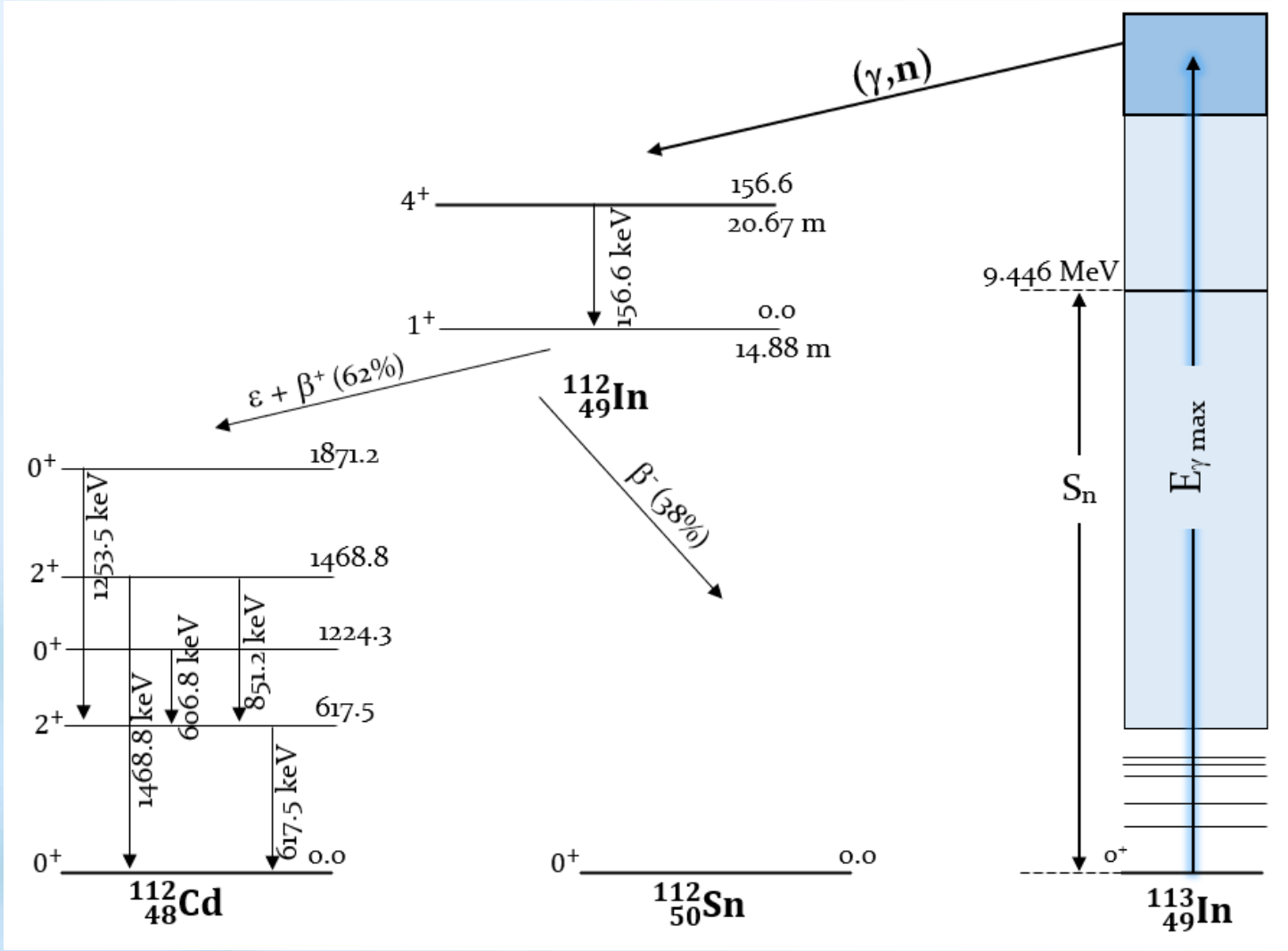

Decay spectrum from an irradiated ^{113}In target

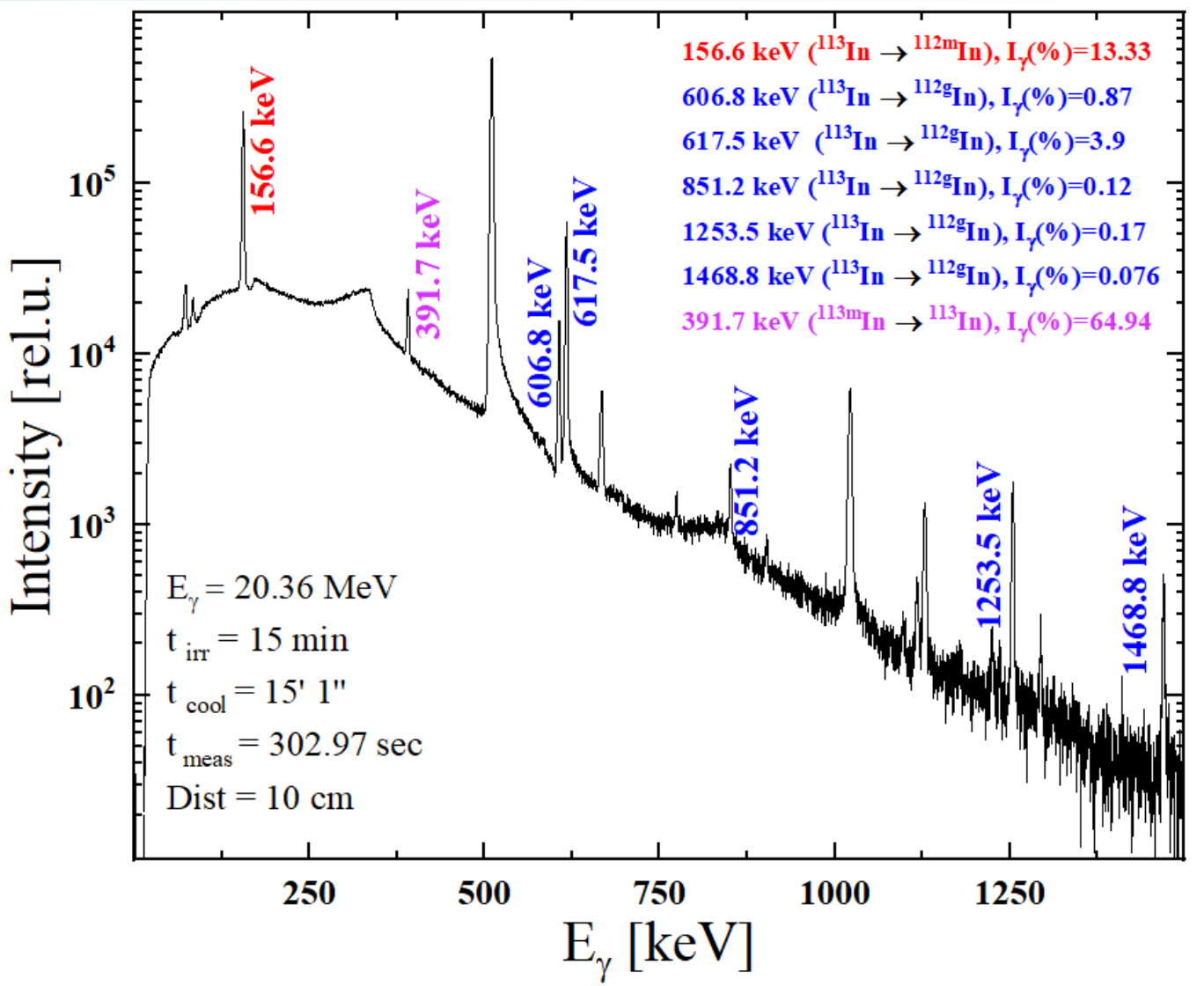

Yields of photoactivation of the ^{113}In nucleus

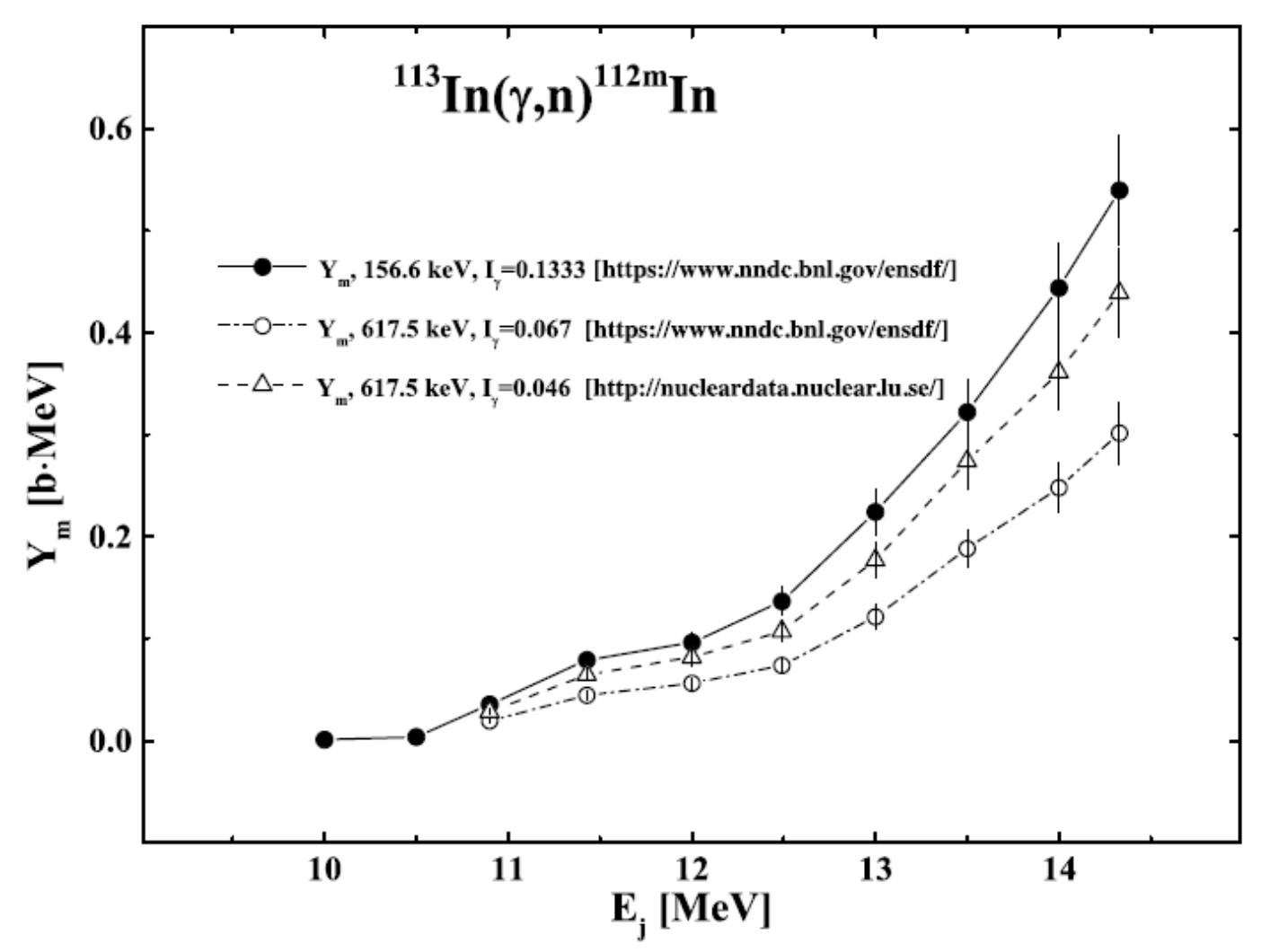

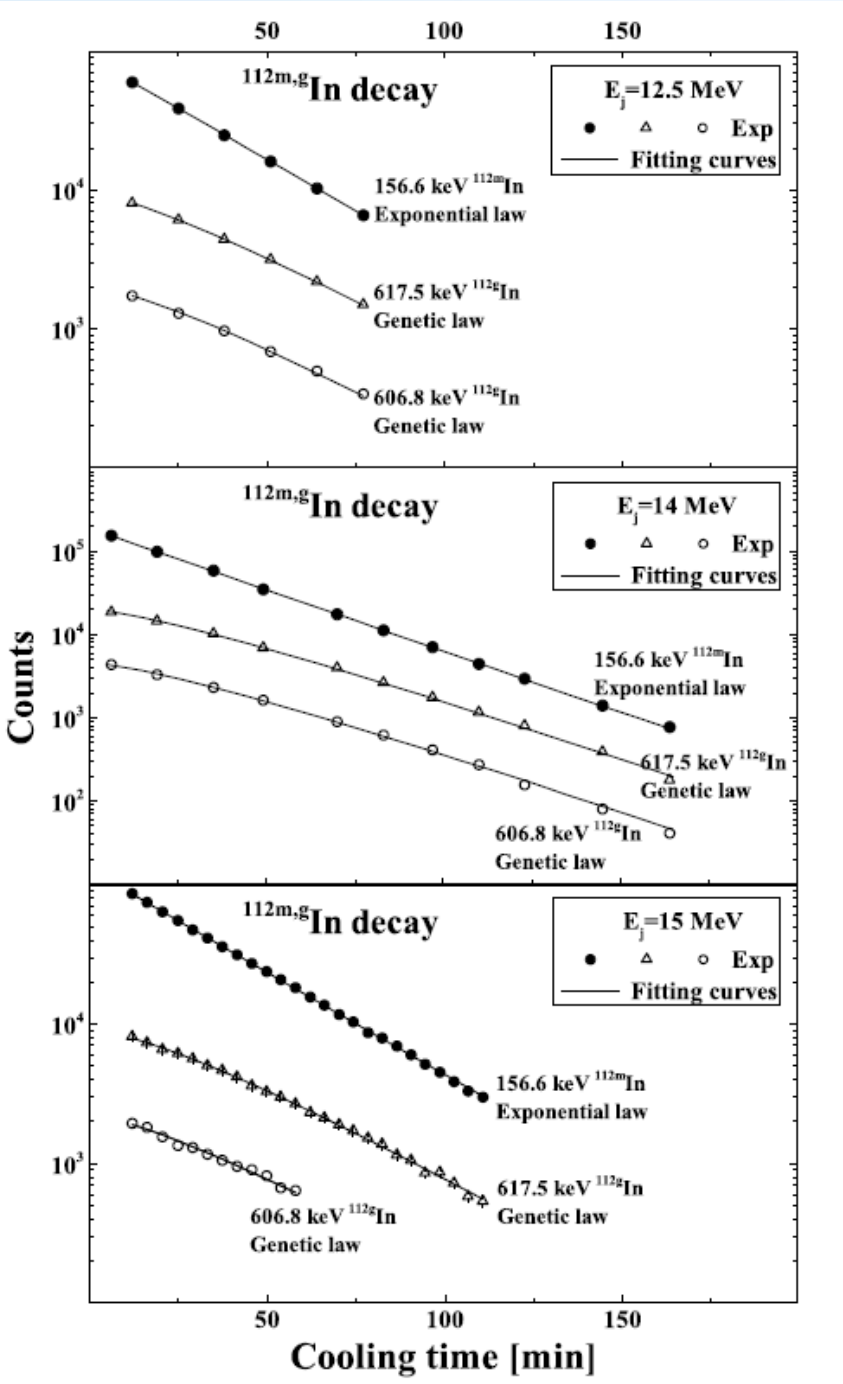

Decay curves constructed from the 156.6 keV (●) γ-line intensities of the 112mIn isomer decay and the 606.8 keV (o) and 617.5 keV (Δ) ones of the 112gIn ground state decay, measured in regular time intervals.

E_γ [keV]	I_γ [%]	
	ENSDF	Our data
606.8	1.6(6)	0.87(9)
617.5	6.7(25)	3.9(4)
851.2	0.21(8)	0.12(2)
1253.5	0.31(12)	0.17(3)
1468.8	0.11(4)	0.076(12)

* I. Semisalov, A. Chekhovska, Ye. Skakun, S. Karpus, V. Kasilov. "Intensities of the strongest γ-ray transitions originating from the ^{112g}In decay determined via photoactivation yield measurements" // Applied Radiation and Isotopes, 2021. Vol. 176. 109843.

Integral cross-sections of photonuclear reactions

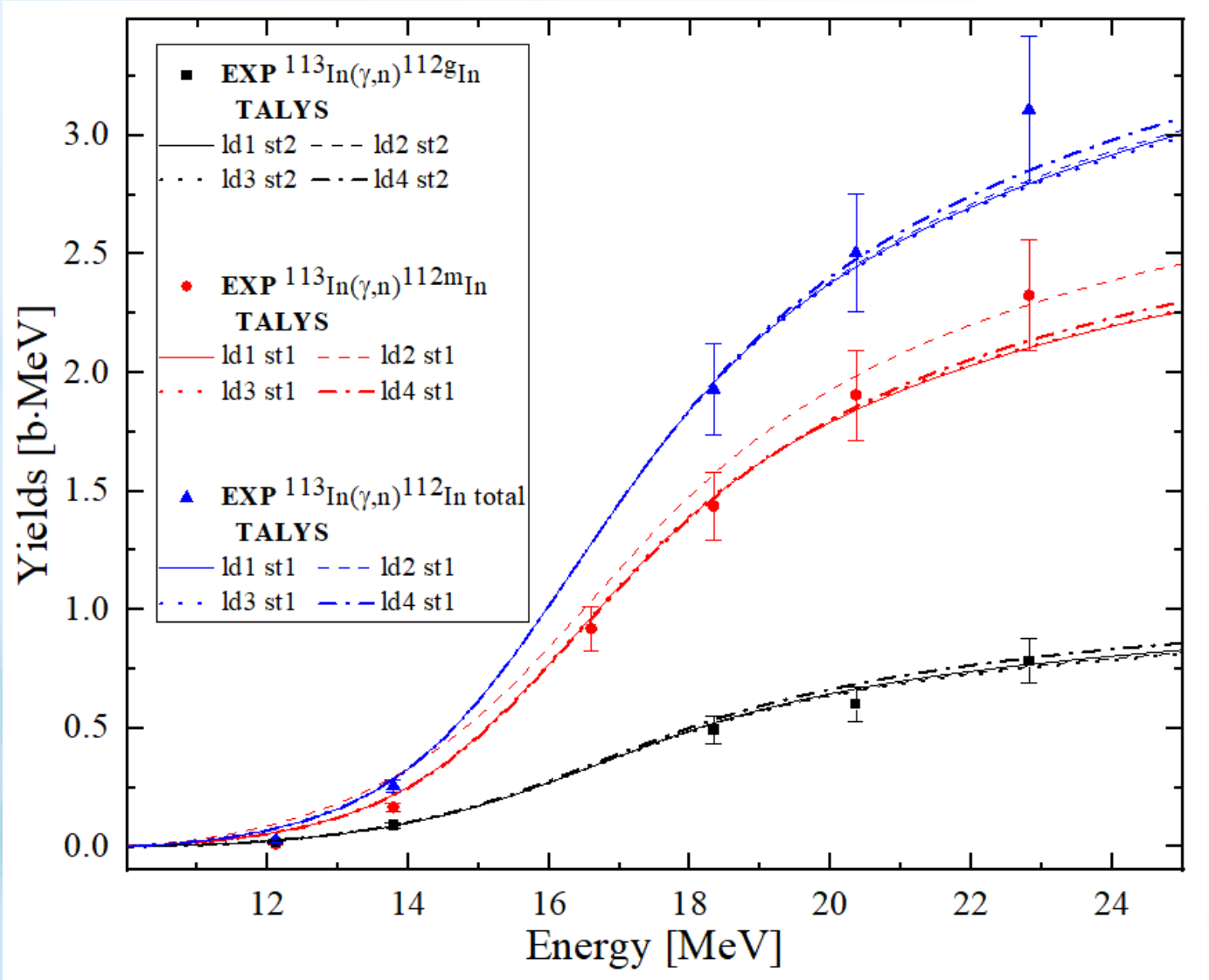

Conclusions

- ✓ **Experimental CS** for $^{112}Sn(\gamma,n)^{111}Sn$, $^{112}Sn(\gamma,p)^{111m}In$, $^{112}Sn(\gamma,p)^{111g}In$, $^{114}Sn(\gamma,n)^{113}Sn$ reactions and comparing data with theoretical predictions according to the statistical theory of nuclear reactions;

- ✓ The **new values of the branching coefficients** of the γ-transitions following the decay of the ^{111}Sn nucleus is determined;

- ✓ An assessment of the correspondence between **theoretical predictions of nuclear RR and experimental data** was made.

FUTURE PLANS:

Experimental data on nuclear reaction cross sections and reaction rates **will be used as input data** for simulating the abundance of chemical elements in the Universe

Thank you all for your time!

Proton enriched nuclei

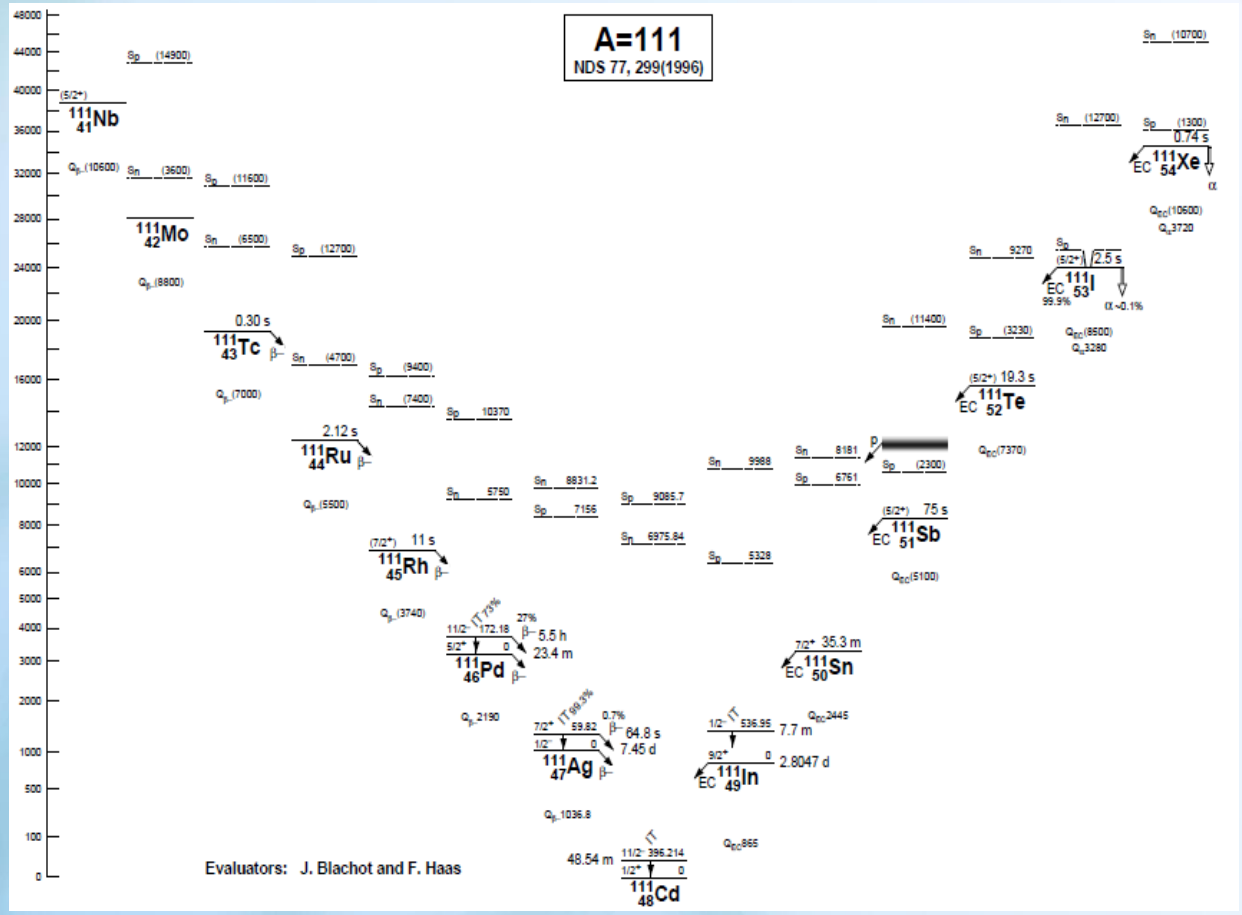

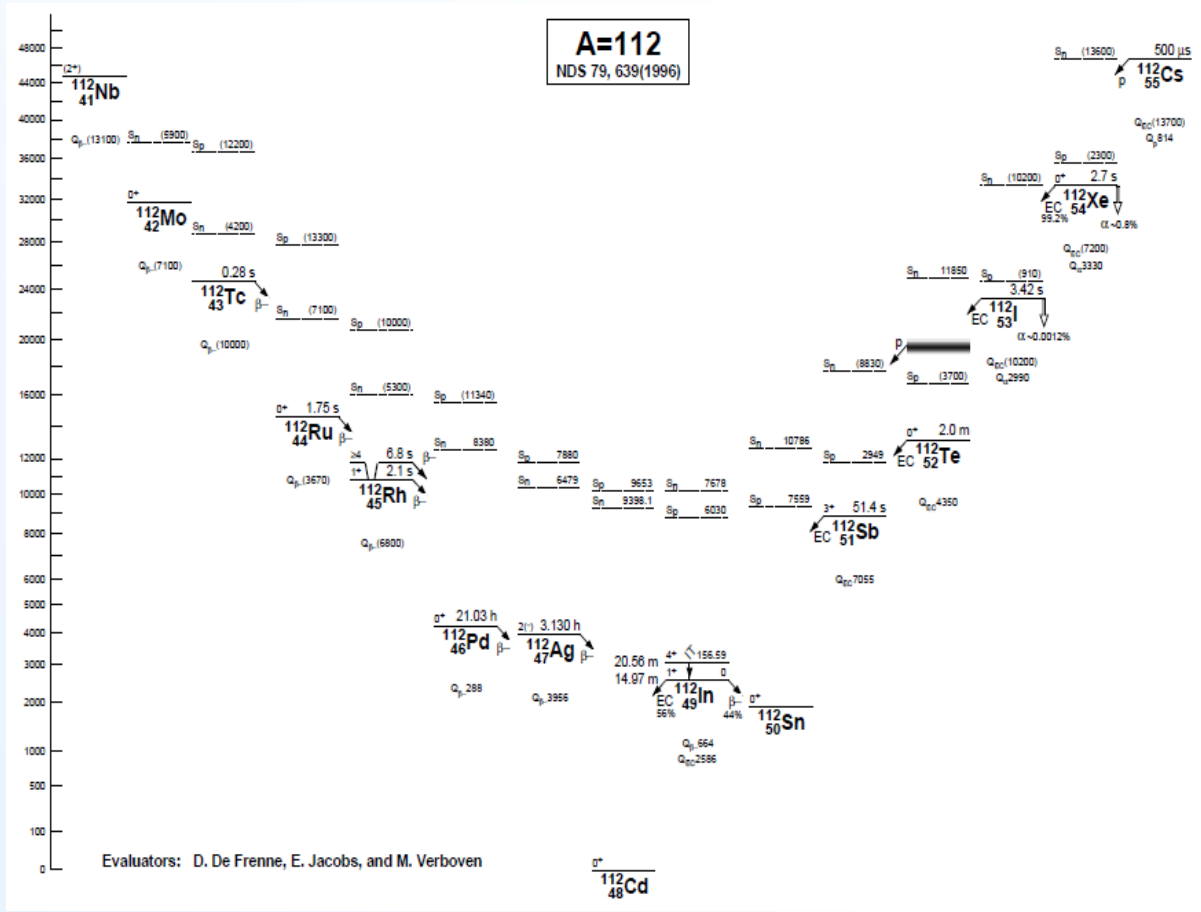

Monitor reaction (standard reaction)
(to determine the flux of incident photons)

Absolute integral yield of the studied reaction

Measured in our experiment, the ratio of the yields of reactions on the ^{112}Sn and ^{197}Au targets

$$Y_{abs}(^{112}Sn) = \frac{Y_{exp}(^{112}Sn)}{Y_{exp}(^{197}Au)} \cdot Y_{abs}(^{197}Au)$$

Absolute integral yield of the monitor reaction

$$Y_{abs}(^{197}Au) = \int_{S_n}^{E_{\gamma\,max}} \sigma(E_\gamma) \cdot \Phi(E_\gamma, E_{\gamma\,max}) dE_\gamma$$

The cross section of the reaction as a function of the energy of the γ-quantum

Energy spectrum of bremsstrahlung with finite energy $E_{\gamma\,max}$

Nuclear reactions in which nuclei were previously obtained

ADOPTED LEVELS, GAMMAS for ^{111}Sn

Author: Jean Blachot | Citation: Nucl. Data Sheets 110, 1239 (2009) | Cutoff date: 1-Feb-2008

Full ENSDF file | Adopted Levels (PDF version)

Q(β-)=-5103 keV *11* S(n)= 8169 keV *15* S(p)= 6758 keV *13* Q(α)= -1374 keV *6*
Reference: 2012WA38

References:

A	^{111}Cd(^{3}He,3nγ),^{108}Cd(α,nγ)	B	^{111}Sb ε decay (75 S)
C	^{112}Sn(p,d)	D	^{112}Sn(^{3}He,αγ)
E	^{112}Sn(pol d,t)	F	^{112}Sn(p,pnγ)
G	(HI,xnγ)	H	^{96}Ru(^{19}F,3PNG)
I	^{98}Mo(^{16}O,3nγ)	J	^{100}Mo(^{20}Ne,A5NG)

ADOPTED LEVELS, GAMMAS for ^{112}In

Authors: S. Lalkovski, F.G. Kondev | Citation: Nucl. Data Sheets 124, 157 (2015) | Cutoff date: 1-Aug-2014

Full ENSDF file | Adopted Levels (PDF version)

Q(β-)=665 keV *4* S(n)= 7671 keV *6* S(p)= 6027 keV *4* Q(α)= -2809 keV *5*
Reference: 2012Wa38

References:

A	^{109}Ag(α,nγ)	B	^{112}In IT decay (20.67 M)
C	^{110}Pd(^{7}Li,5nγ)	D	^{110}Cd(α,NPG)
E	^{110}Cd(α,d)	F	^{111}Cd(^{3}He,d)
G	^{112}Cd(p,nγ)	H	^{112}Cd(d,2nγ)
I	^{113}In(p,d)	J	^{113}In(d,t)
K	^{113}In(γ,XN)	L	^{100}Mo(^{16}O,p3nγ)

ADOPTED LEVELS, GAMMAS for ^{113}Sn

Author: Jean Blachot | Citation: Nucl. Data Sheets 111, 1471 (2010) | Cutoff date: 1-May-2009

Full ENSDF file | Adopted Levels (PDF version)

Q(β-)=-3911 keV *18* S(n)= 7743.6 keV *16* S(p)= 7626 keV *5* Q(α)= -2248.8 keV *23*
Reference: 2012WA38

References:

A	^{113}Sn IT decay (21.4 M)	B	^{113}Sb ε decay
C	^{110}Cd(α,nγ)	D	^{111}Cd(α,2nγ)
E	^{112}Cd(α,3nγ)	F	^{112}Sn(n,γ) E=95 EV
G	^{112}Sn(d,p),^{114}Sn(d,t)	H	^{113}In(p,nγ)
I	^{113}In(p,3nγ)	J	^{114}Sn(p,d)
K	^{115}Sn(p,t)	L	^{114}Sn(p,d) IAS
M	^{100}Mo(^{18}O,5nγ)		

Bremsstrahlung radiation

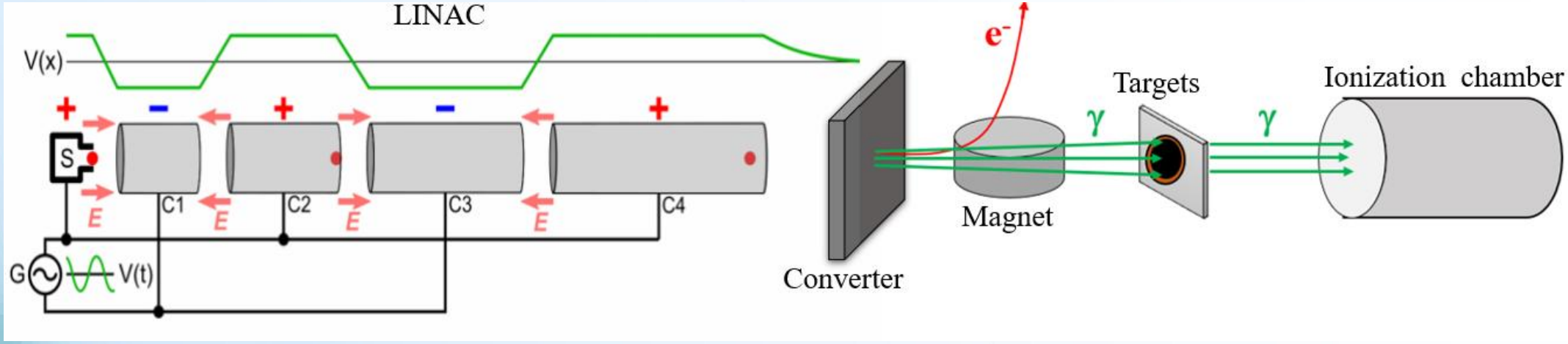

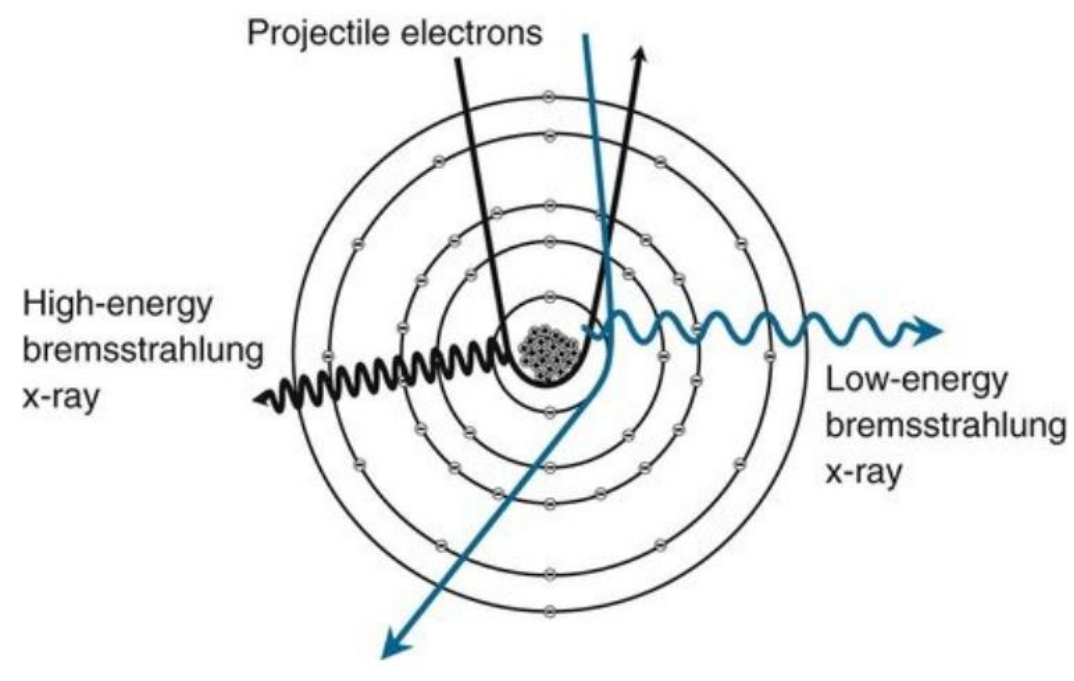

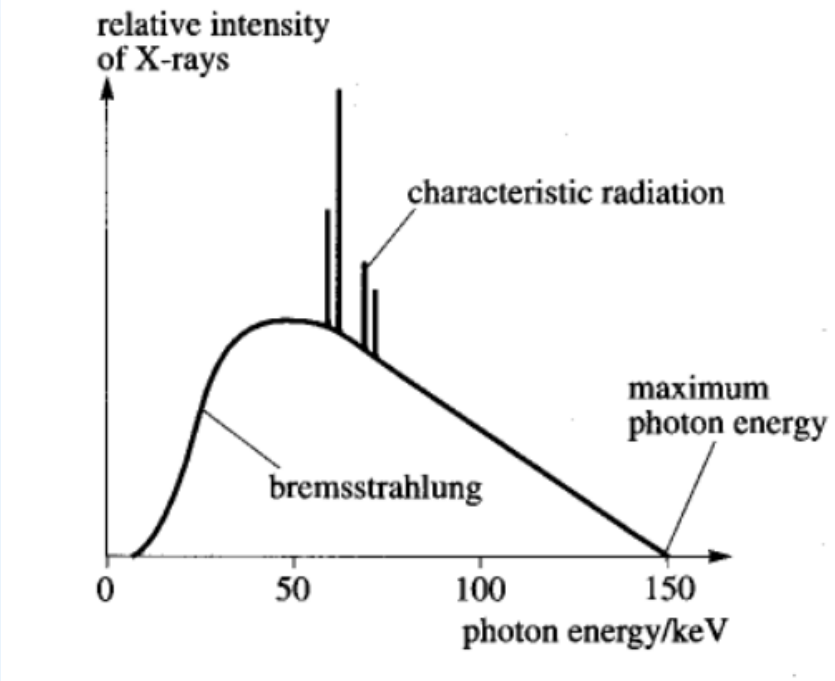

Microtron MT-25

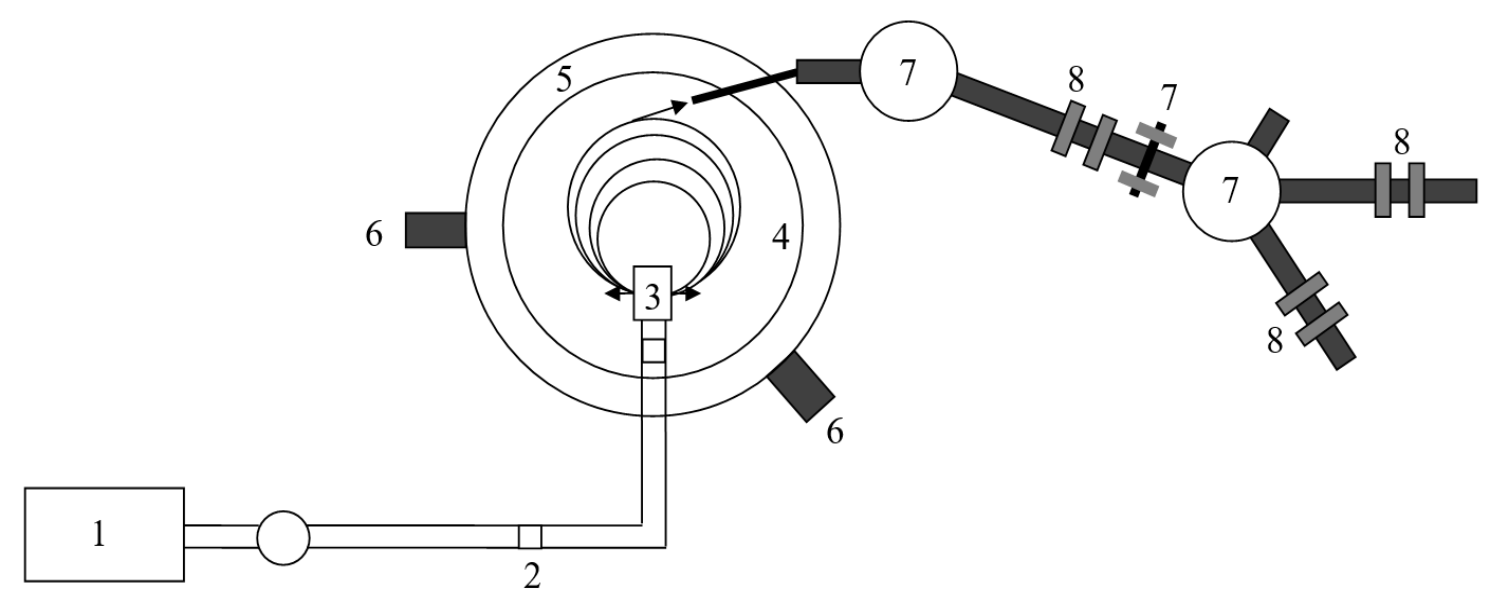

1. Magnetron, **2.** Circulator with Water Load,

3. Accelerating Cavity, **4.** Vacuum Chamber,

5. Pot-Shaped Magnet, **6.** Vacuum Pump,

7. Deflectors, **8.** Quadrupole Lens.

1. Microtron, **2.** Convertor (with two W targets 1.5 and 3 mm and one Sn foil 0.2 mm),

3. Target with combined Al-Cu scattering foils,

4. Primary conical stainless steel collimator,

5. Secondary square W-steel collimator,

6. Water-cooled chamber, **7.** Research target,

8. Monitor target (Cu or Au),

9. Absorber.

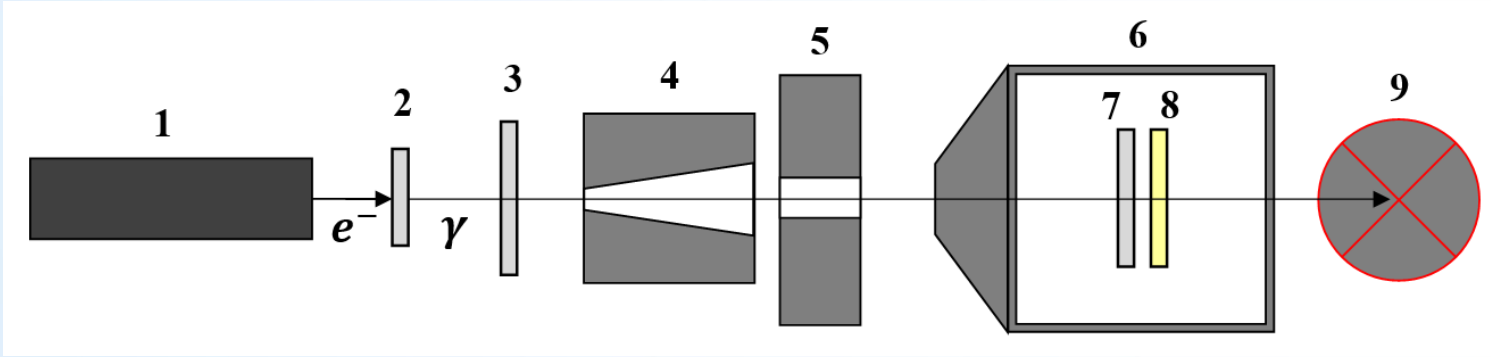

Nuclear Physics Institute of the Czech Academy of Sciences
Department of Accelerators, Prague
Microtron MT-25

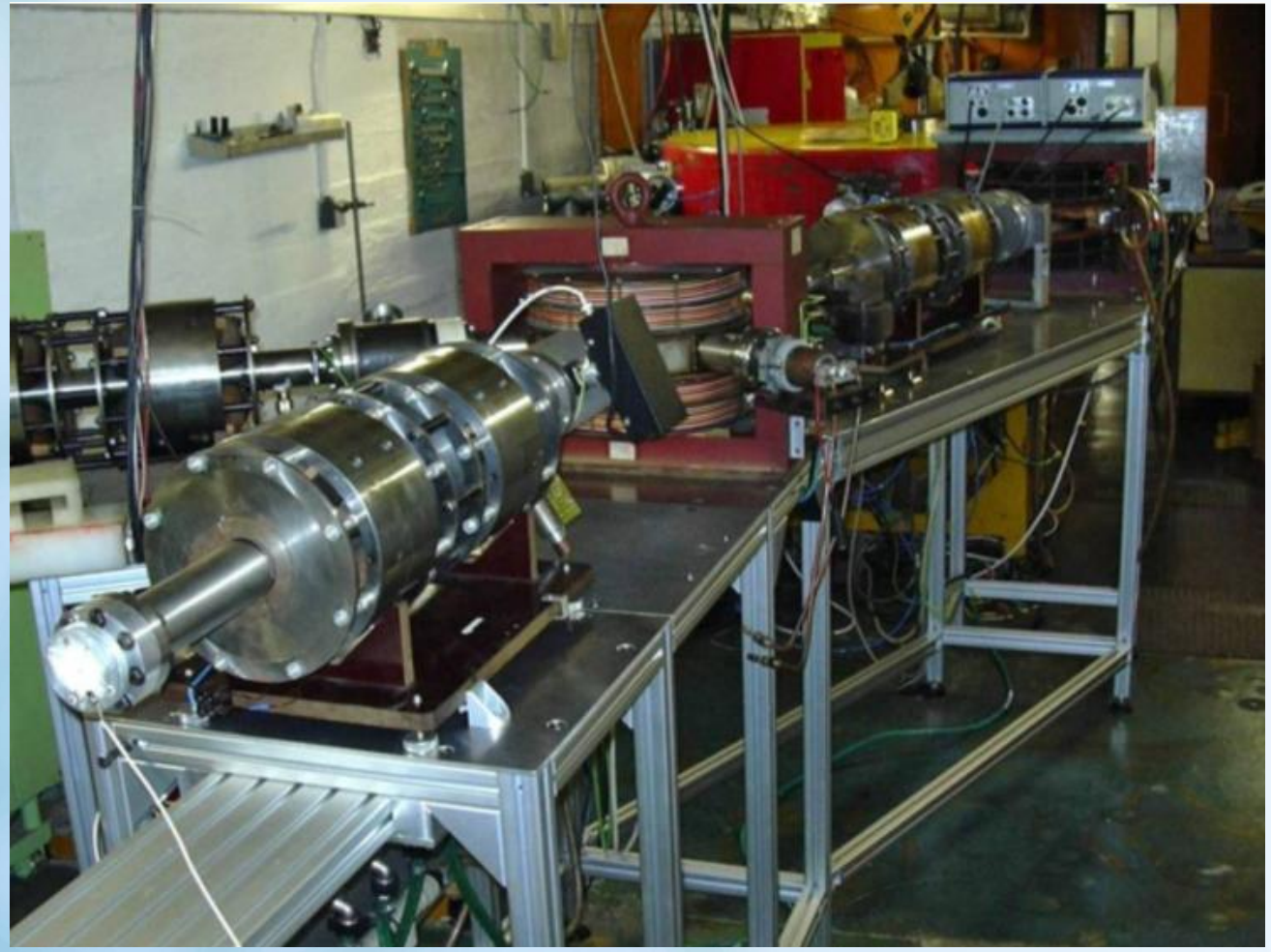

Basic parameters:

Maximum energy	25 MeV
Energy range	6 - 25 MeV
Electron current	25 μA
High frequency source	
Tunable magnetron	2 790 ± 5 MHz
Peak power	3 MW
Pulse lenght	3 μs
Repetition rate	425 s^{-1}
Resonator freq.	2 796 MHz
Power supply freq.	50 Hz

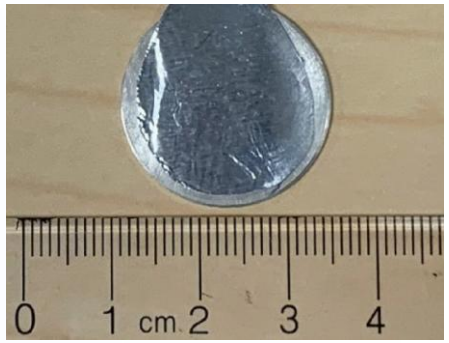

Target	Enrichment	Weight
Sn	nat	0.320
^{112}Sn	80%	0.077
^{114}Sn	83%	0.194
^{113}In	66%	0.072
^{197}Au	nat	0.030